AN INVESTIGATION TOWARDS STRUCTURE PRESERVING TRANSIENT STABILITY ANALYSIS USING ENERGY FUNCTIONS

by

Ravi Shankar Buyyanapragada

A thesis submitted to the faculty of
The University of North Carolina at Charlotte
in partial fulfillment of the requirements
for the degree of Master of Science in
Electrical Engineering

Charlotte

2015

Approved by:

_____
Dr. Sukumar Kamalasadan

_____
Dr. Valentina Cecchi

_____
Dr. Bharat Joshi

ABSTRACT

RAVI SHANKAR BUYYANAPRAGADA. An investigation towards structure preserving transient stability analysis using energy functions (Under the direction of Dr. SUKUMAR KAMALASADAN)

This thesis investigates transient stability of the power system using numerical methods and direct methods. Structure preserving models are prepared for the stability analysis, where all nodes in the system are considered. Moreover, frequency dependent loads are modeled to analyze the effect of dynamic loads on the transient stability of the power system. Center of inertia reference frame was used for measuring relative rotor angles. Additionally, Structure preserving energy functions are developed, where all buses of the power system are considered without eliminating buses where current injection are zero and loads are modeled as frequency dependent loads. The structure preserving energy functions developed are used to calculate potential energy, kinetic energy and total energy of the system and stability of the system was predicted by looking at the change in kinetic energy and potential energy. Moreover, the critical clearing time (CCT) was predicted using potential energy boundary surface method (PEBS), where critical clearing time is equal to the time at which total energy is equal to potential energy. Standard IEEE test systems like western system coordinating council (WSCC), New England 39 bus system and NETS-NYPS 68 bus system are used for benchmarking.

ACKNOWLEDGEMENTS

This thesis would not have been possible without the guidance and help of several individuals who in one way or another contributed and extended their valuable assistance in the preparation and completion of this study.

First and foremost, I would like to express my utmost gratitude to my advisor, Dr. Sukumar Kamalasadan for his valuable guidance and selfless support during these two years of my master's studies. His patience and unfailing encouragement have been the major contributing factors in the completion of my thesis research.

It gives me immense pleasure in expressing my hearty gratitude to Dr. Sudipta Ghosh for his intensive and sincere guidance throughout the period of my research work. I am heartfelt thankful to my family and friends for their never ending love and support.

I sincerely thank the committee members Dr. Valentina Cecchi and Dr. Bharat Joshi for taking time to be on my committee and assess my work.

Finally, I would like to thank all the professors and staff at the University of North Carolina At Charlotte who contributed in providing quality education.

TABLE OF CONTENTS

LIST OF FIGURES

CHAPTER 1 : INTRODUCTION

This chapter presents a brief introduction and the organization of the thesis. Section 1.1 Section 1.2 Section 1.3 presents brief overview and classification of power system stability. Importance of power system stability is presented in Section 1.4. Section1.5 presents the organization of thesis.

1.1. Overview

The function of an electric power system is to convert energy from one of the naturally available forms to the electrical form and to transport it to the points of consumptions. Energy is seldom consumed in the electrical form but is rather converted to other forms such as heat, light, and mechanical energy. The advantage of the electrical form of energy is that it can be transported and controlled with relative ease and with a high degree of efficiency and reliability [1]. Modern electric power systems have three separate components - generation, transmission and distribution. Electric power is generated at the power generating stations by synchronous alternators that are usually driven either by steam or hydro turbines. Most of the power generation takes place at generating stations that may contain more than one such alternator-turbine combination. Depending upon the type of fuel used, the generating stations are categorized as thermal, hydro, nuclear etc. Many of these generating stations are remotely located. Hence the electric power generated at any such station has to be transmitted over a long distance to load centers that are usually cities or towns. This is called the power transmission. Modern day power systems are

complicated networks with hundreds of generating stations and load centers being interconnected through power transmission lines. Electric power is generated at a frequency of either 50 Hz or 60 Hz [2].

1.2. Power System Stability

Power system stability may be broadly defined as that property of a power system that enables it to remain in a state of operating conditions and to regain an acceptable state of equilibrium after being subjected to a disturbance. Instability in a power system may be manifested in many different ways depending on the system configuration and operating mode. Traditionally, the stability problem has been one if maintaining synchronous operation. Since power systems rely on synchronous machines for generation of electrical power, a necessary condition for satisfactory system operation is that all synchronous machines remain in synchronism or in step. This aspect of stability is influenced by the dynamics of generator rotor angles and power-angle relationships. In the evaluation of stability the concern is the behavior of the power system when subjected to a transient disturbance. The disturbance may be small or large. Small disturbances in the form of load changes take place continually, and the system adjusts itself to the changing condition. The system must be able to operate satisfactorily under these conditions and successfully supply the maximum amount of load [1].

1.3. Classification of Stability

Power system stability is essentially a single problem. However, the various forms of instabilities that a power system may undergo cannot be properly understood and effectively dealt with by treating it as such [3]. Analysis of stability, including identifying key factors that contribute to instability and devising methods of improving stable

operation, is greatly facilitated by classification of stability into appropriate categories [1]. Figure 1.1 [1] provides a categorization of power system stability. There are two main categories of power system stability: angle stability and voltage stability. Angle stability has two main subclasses: small signal (steady state) stability and transient stability. Voltage stability also has two main subclasses: Large disturbance voltage stability and small disturbance voltage stability.

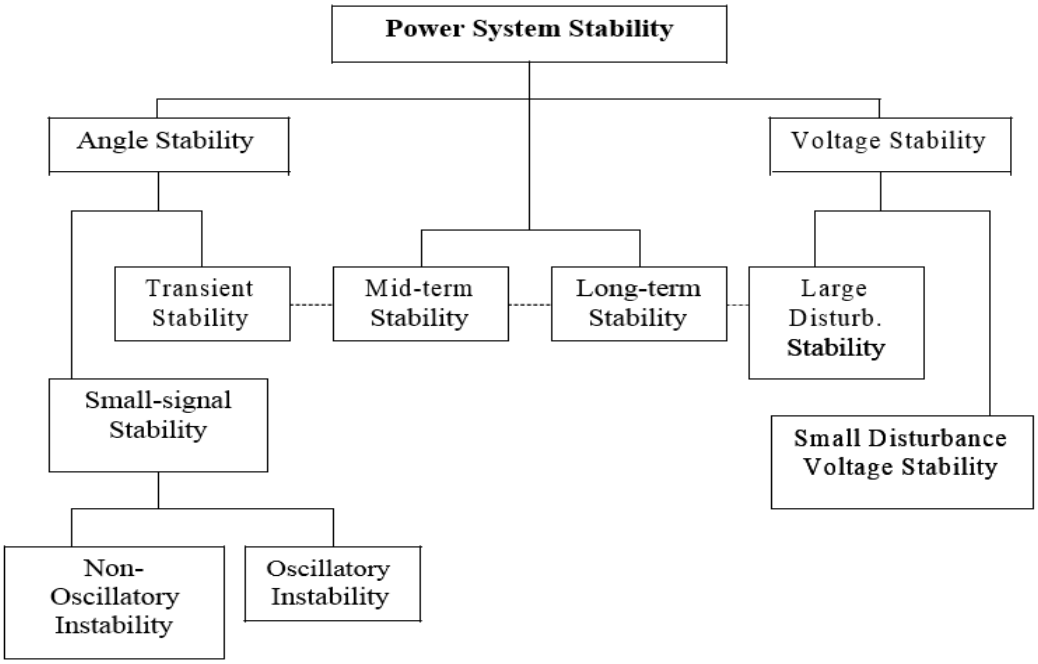

FIGURE 1.1: Classification of stability

1.3.1. Rotor Angle Stability

Rotor angle stability refers to the ability of synchronous machines of an interconnected power system to remain in synchronism after being subjected to a disturbance [3]. It depends on the ability to maintain/restore equilibrium between electromagnetic torque and mechanical torque of each synchronous machine in the system. Instability that may result occurs in the form of increasing angular swings of some generators leading to their loss of synchronism with other generators. The rotor

angle stability problem involves the study of the electromechanical oscillations inherent in power systems. A fundamental factor in this problem is the manner in which the power outputs of synchronous machines vary as their rotor angles change. Under steady-state conditions, there is equilibrium between the input mechanical torque and the output electromagnetic torque of each generator, and the speed remains constant. If the system is perturbed, this equilibrium is upset, resulting in acceleration or deceleration of the rotors of the machines according to the laws of motion of a rotating body. If one generator temporarily runs faster than another, the angular position of its rotor relative to that of the slower machine will advance. The resulting angular difference transfers part of the load from the slow machine to the fast machine, depending on the power-angle relationship. This tends to reduce the speed difference and hence the angular separation. The power-angle relationship is highly nonlinear. Beyond a certain limit, an increase in angular separation is accompanied by a decrease in power transfer such that the angular separation is increased further. Instability results if the system cannot absorb the kinetic energy corresponding to these rotor speed differences. For any given situation, the stability of the system depends on whether or not the deviations in angular positions of the rotors result in sufficient restoring torques [1]. Loss of synchronism can occur between one machine and the rest of the system, or between groups of machines, with synchronism maintained within each group after separating from each other [3]. The change in electromagnetic torque of a synchronous machine following a perturbation can be resolved into two components:

• Synchronizing torque component, in phase with rotor angle deviation.

• Damping torque component, in phase with the speed deviation

System stability depends on the existence of both components of torque for each of the synchronous machines. Lack of sufficient synchronizing torque results in aperiodic or non-oscillatory instability, whereas lack of damping torque results in oscillatory instability.

1.3.2. Small-Disturbance (or Small-Signal) Rotor Angle Stability

Small-disturbance (or small-signal) rotor angle stability is concerned with the ability of the power system to maintain synchronism under small disturbances. The disturbances are considered to be sufficiently small that linearization of system equations is permissible for purposes of analysis [4].

- Small-disturbance stability depends on the initial operating state of the system. Instability that may result can be of two forms: i) increase in rotor angle through a non-oscillatory or aperiodic mode due to lack of synchronizing torque, or ii) rotor oscillations of increasing amplitude due to lack of sufficient damping torque [3]. In today's power systems, small-disturbance rotor angle stability problem is usually associated with insufficient damping of oscillations. The aperiodic instability problem has been largely eliminated by use of continuously acting generator voltage regulators; however, this problem can still occur when generators operate with constant excitation when subjected to the actions of excitation limiters (field current limiters) [3]. Small-disturbance rotor angle stability problems may be either local or global in nature. Local problems involve a small part of the power system, and are usually associated with rotor angle oscillations of a single power plant against

the rest of the power system. Such oscillations are called local plant mode oscillations. Global problems are caused by interactions among large groups of generators and have widespread effects. They involve oscillations of a group of generators in one area swinging against a group of generators in another area. Such oscillations are called interarea mode oscillations. Their characteristics are very complex and significantly differ from those of local plant mode oscillations. Load characteristics, in particular, have a major effect on the stability of interarea modes [1]. - The time frame of interest in small-disturbance stability studies is on the order of 10 to 20 seconds following a disturbance.

1.3.3. Transient Stability

Large-disturbance rotor angle stability or transient stability, as it is commonly referred to, is concerned with the ability of the power system to maintain synchronism when subjected to a severe disturbance, such as a short circuit on a transmission line. The resulting system response involves large excursions of generator rotor angles and is influenced by the nonlinear power-angle relationship [3]. Transient stability depends on both the initial operating state of the system and the severity of the disturbance. Instability is usually in the form of aperiodic angular separation due to insufficient synchronizing torque, manifesting as first swing instability. However, in large power systems, transient instability may not always occur as first swing instability associated with a single mode, it could be a result of superposition of a slow interarea swing mode and a local-plant swing mode causing a large excursion of rotor angle beyond the first swing [1]. The time frame of interest in transient stability studies

is usually 3 to 5 seconds following the disturbance. It may extend to 10–20 seconds for very large systems with dominant inter-area swings.

1.3.4. Voltage Stability

Voltage stability refers to the ability of a power system to maintain steady voltages at all buses in the system after being subjected to a disturbance from a given initial operating condition. It depends on the ability to maintain/restore equilibrium between load demand and load supply from the power system. Instability that may result occurs in the form of a progressive fall or rise of voltages of some buses. A possible outcome of voltage instability is loss of load in an area, or tripping of transmission lines and other elements by their protective systems leading to cascading outages. Loss of synchronism of some generators may result from these outages or from operating conditions that violate field current limit [5]. Progressive drop in bus voltages can also be associated with rotor angle instability. For example, the loss of synchronism of machines as rotor angles between two groups of machines approach 180 causes rapid drop in voltages at intermediate points in the network close to the electrical center [1]. The driving force for voltage instability is usually the loads. A major factor contributing to voltage instability is the voltage drop that occurs when active and reactive power flow through inductive reactances of the transmission network, this limits the capability of the transmission network for power transfer and voltage support [3].

- Large-disturbance voltage stability refers to the system's ability to maintain steady voltages following large disturbances such as system faults, loss of generation, or circuit contingencies. This ability is determined by the system

and load characteristics, and the interactions of both continuous and discrete controls and protections. Determination of large-disturbance voltage stability requires the examination of the nonlinear response of the power system over a period of time sufficient to capture the performance and interactions of such devices as motors, underload transformer tap changers, and generator field-current limiters. The study period of interest may extend from a few seconds to tens of minutes [3].

- Small-disturbance voltage stability refers to the system's ability to maintain steady voltages when subjected to small perturbations such as incremental changes in system load. This form of stability is influenced by the characteristics of loads, continuous controls, and discrete controls at a given instant of time. This concept is useful in determining, at any instant, how the system voltages will respond to small system changes. With appropriate assumptions, system equations can be linearized for analysis thereby allowing computation of valuable sensitivity information useful in identifying factors influencing stability [3].

1.3.5. Frequency Stability

Frequency stability refers to the ability of a power system to maintain steady frequency following a severe system upset resulting in a significant imbalance between generation and load. It depends on the ability to maintain/restore equilibrium between system generation and load, with minimum unintentional loss of load. Instability that may result occurs in the form of sustained frequency swings leading to tripping of generating units and/or loads [1].

1.4. Importance of Power System Stability Studies

Power system engineering forms a vast and major portion of electrical engineer studies. It is mainly concerned with the production of electrical power and its transmission from the sending end to the receiving end as per consumer requirements, incurring minimum amount of losses. The power at the consumer end is often subjected to changes due to the variation of load or due to disturbances induced within the length of transmission line. For this reason the term power system stability is of utmost importance in this field, and is used to define the ability of the of the system to bring back its operation to steady state condition within minimum possible time after having undergone some sort of transience or disturbance in the line. Ever since the 20th century, till the recent times all major power generating stations over the globe has mainly relied on A.C. distribution system as the most effective and economical option for the transmission of electrical power. Even the most effective way to produce bulk amount of power has been with the evolution of A.C. machine (i.e. alternator or synchronous generator). In the power plants, several synchronous generators with different voltage ratings are connected to the bus terminals having the same frequency and phase sequence as the generators, while the consumer ends are feeded directly from those bus terminals. And therefore for stable operation it is important for the bus to be well synchronized with the generators over the entire duration of transmission, and for this reason the power system stability is also referred to as synchronous stability and is defined as the ability of the system to return to synchronism after having undergone some disturbance.

1.5. Organization of Thesis

This section presents overview of the organization of thesis as follows.

Chapter 1: Introduction

This chapter starts by stressing the basic concepts of power system stability in Section 1.2. Section1.3 presents classification of stability, and brief overview of rotor angle stability, small signal stability, transient stability, voltage stability and frequency stability. Section 1.4 presents the importance of power system stability studies and Section 1.5 presents the organization of thesis.

Chapter 2: Existing Methods for Transient Stability Analysis

In this chapter, a detailed review of existing methods for transient stability studies are presented. Section 2.1 and Section 2.2 presents swing equation and equal area criterion method. Section 2.3 explains various numerical integration methods used for time domain analysis. Section 2.4 explains the concept of direct methods and its application for transient stability analysis.

Chapter 3: Synchronous Machine Models for Stability Studies

In this chapter, various synchronous machine models available for stability studies are presented. In Section 3.2 and Section 3.3 equations related to classical and detailed models are presented. Section 3.4 and Section 3.5 explains the concepts of synchronous reference frame and center of inertia reference frame (COI). In Section 3.6 multi machine models for transient stability are presented and Section 3.7 presents the test system used for simulations and analyzes simulation results.

Chapter 4: Transient Stability Studies Using Direct Methods

In this chapter, application of direct methods for transient stability analysis is explained in detail. In section 4.2, Lyapunov's method is presented and in Section 4.3, mathematical equations are presented for multi machine power system. Moreover, simulation results and its analysis are presented.

Chapter 5: Structure Preserving Energy Functions based transient stability using direct methods.

In this chapter, concepts of structure preserving networks are explained. In section 5.2, use of structure preserving models for multi machine transient stability studies are explained .Section 5.3 explains the effect of load models on power system stability. In Section 5.4, mathematical equations for structure preserving network with frequency dependent loads are presented. Section 5.5 and Section 5.6 presents simulation results and its analysis.

Chapter 6: Future Work and Conclusions

CHAPTER 2 : EXISTING METHODS FOR TRANSIENT STABILITY ANALYSIS

This chapter presents a review of existing methods for transient stability analysis. Section 2.1 presents swing equation. Section 2.2 presents equal area criterion. Various methods for transient stability analysis are presented in Section 2.3 Section 2.4. Section 2.5 presents summary.

2.1. Swing Equation

Under normal operating conditions, the relative position of the rotor axis and the resultant magnetic field axis is fixed. The angle between the two is known as power angle or torque angle. During any disturbance, rotor will decelerate or accelerate with respect to the synchronously rotating air gap mmf, and a relative motion begins. The equation describing this relative motion is known as swing equation. If, after this oscillatory period, the locks back into synchronous speed, the generator will maintain its stability. If the disturbance does not involve any net change in power, the rotor returns to its original position. If the disturbance is created by a change in generation, load, or in network conditions, the rotor comes to a new operating power angle relative to the synchronously revolving field [6].

Consider a synchronous generator developing an electromagnetic torque T_e and running at the synchronous speed w_{sm}. If T_m is the driving mechanical torque, then under steady state operation with losses neglected we have

$$T_m = T_e \tag{2.1}$$

A departure from steady state due to a disturbance results in an accelerating ($T_m > T_e$) or deceleration ($T_m < T_e$) torque T_a on the rotor.

$$T_a = T_m - T_e \tag{2.2}$$

If J is the combined moment of inertia of the prime mover and generator, neglecting frictional and damping torques, from law's of rotation we have

$$J\frac{d^2\theta m}{dt^2} = T_a = T_m - T_e \tag{2.3}$$

Where θ_m is the angular displacement of the rotor with respect to the stationary reference axis on the stator. Since we are interested in the rotor speed relative to synchronous speed, the angular reference is chosen relative to a synchronously rotating reference frame moving with angular velocity w_{sm}, that is

$$\theta_m = w_{sm}t + \delta_m \tag{2.4}$$

Where δ_m is the rotor position before disturbance at time t = 0, measured from the synchronously rotating reference frame.

Swing equation in terms of the per unit (p.u)

$$\frac{2H}{w_s}\frac{d^2\delta}{dt^2} = P_{m\,(pu)} - P_{e\,(pu)} \tag{2.5}$$

If (2.5) is expressed in terms of frequency f_0 and δ is expressed in electrical degrees, the swing equation becomes

$$\frac{H}{180f_0}\frac{d^2\delta}{dt^2} = P_{m\,(pu)} - P_{e\,(pu)} \tag{2.6}$$

Where $$H = \frac{kinectic\ energy\ in\ MJ\ at\ rated\ speed}{machine\ rating\ in\ MVA} = \frac{W_K}{S_B} \tag{2.7}$$

2.2. Equal Area Criterion

A method known as equal area criterion can be used for quick prediction of stability. This method is based on graphical interpretation of the energy stored in the rotating mass as an aid to determine if the machine maintains its stability after a disturbance. The method is only applicable to one machine connected to an infinite bus or a two machine system [6].Consider a single-machine infinite-bus (SMIB) system of Figure 2.2. Assume that the system is a purely reactive, a constant P_m and constant voltage behind transient reactance for the system in Figure 2.2.

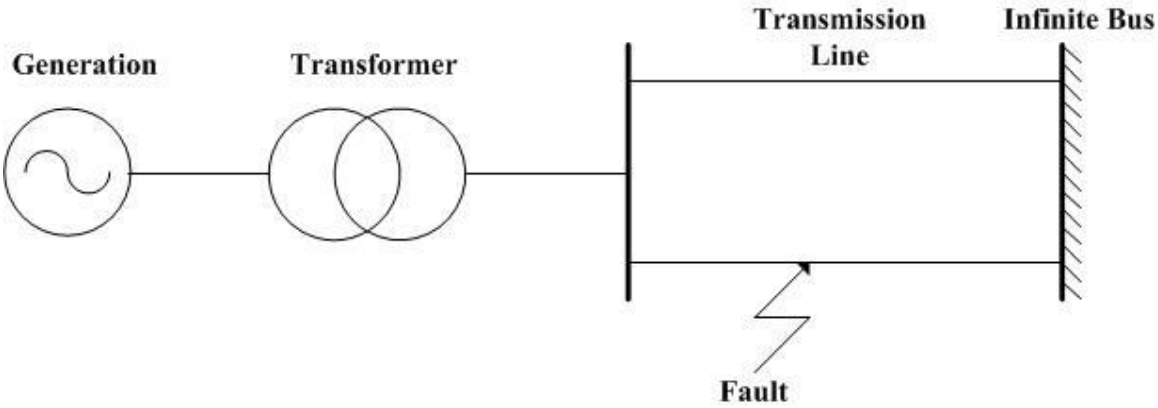

FIGURE 2.1: Single machine infinite bus system [7].

Assume that a 3-phase fault appears in the system at $t = 0$ and it is cleared by opening one of the lines. The power angle characteristics of the system are shown in Figure 2.3.

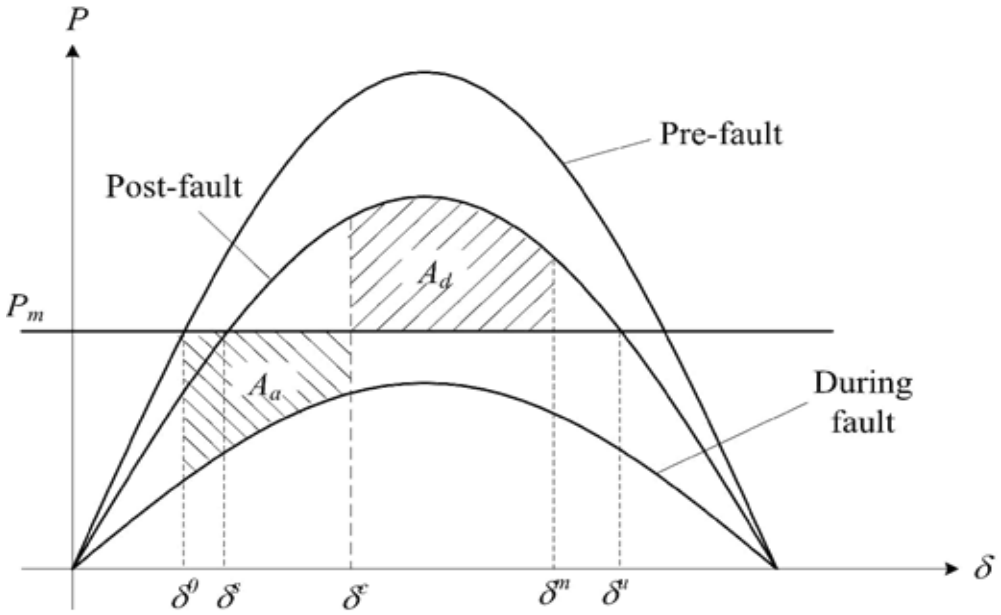

FIGURE 2.2: Power-Angle Characteristic of the System in Fig. 2.7 [8].

Let δ^0 and δ^s be the pre-fault and post-fault operating or stable-equilibrium points, respectively, of the system. During the fault, the electrical output P_e of the generator reduces drastically (almost to zero) but the mechanical power P_m remains almost constant. Thus the generator accelerates and its angle δ increases. When the fault is cleared by disconnecting the faulted line at time t_c, the output power of the generator becomes greater than the mechanical power and the generator decelerates to bring its speed to normal as shown in Figure 2.3. If the system is stable, the generator will recover to its steady-state speed (or zero speed deviation) at some peak angle δ^m. At δ^m, $P_e > P_m$ and the generator will continue to decelerate. The angle δ decreases from δ^m and reaches a minimum value below δ^s before it starts to increase again. The generator angle will oscillate around δ^s and eventually it will settle down at δ^s because of the system damping. For a given clearing angle δ^c, the peak angle δ^m can be determined by equating the accelerating area A_a to decelerating area A_d. The expressions for A_a and A_d are

$$A_a = \int_{\delta^0}^{\delta^c} (P_m - P_e^f)\, d\delta \tag{2.8}$$

$$A_d = \int_{\delta^c}^{\delta^m} (P_e^p - P_m)\, d\delta \tag{2.9}$$

Where

P_e^f is the during-fault electrical power

P_e^p is the post-fault electrical power

For a system to be transient stable, the maximum decelerating area is greater than the accelerating area. That is, $A_d > A_a$. For a clearing time t_c when $A_d = A_a$, we reach the maximum clearing time referred to as the critical clearing time t_{cr}.

2.3. Numerical Integration Methods

Numerical integration techniques can be applied to obtain approximate solutions of nonlinear differential equations. Many algorithms are available for numerical integration such as Euler's method of integration, Modified Euler's method of integration, Runga Kutta method. Euler's method is the simplest and the least accurate method of all numerical methods [6]. The time-domain numerical integration is not suitable for on-line security analysis due to the long CPU run times for simulation. A typical time-domain numerical integration of 2 seconds takes more than 120 seconds depending on the step size of the integration. Larger step size that reduce time causes inaccurate and less reliable results than smaller step size [7].

2.3.1. Euler's Method

Consider the first-order differential equation

$$\frac{dy}{dx} = f(x, t) \tag{2.10}$$

With $x = x_0$ at $t = t_0$ figure illustrates the principle of applying the Euler method.

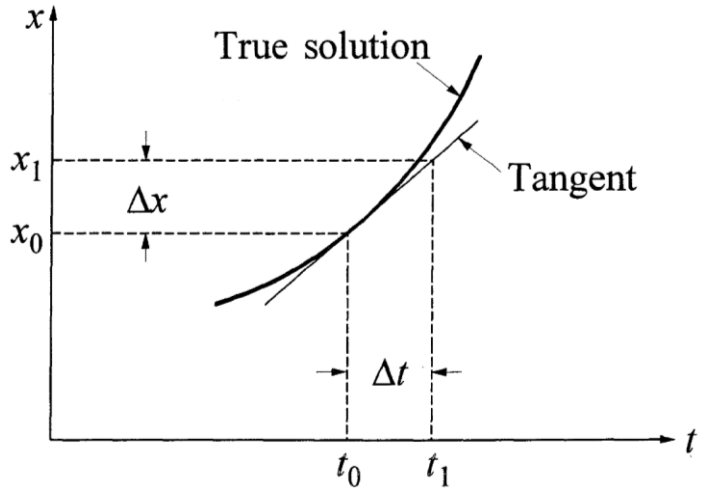

FIGURE 2.3: Euler's method

At $= x_0$, $t = t_0$ we can approximate the curve representing the true solution but its tangent having a slope

$$\left.\frac{dx}{dt}\right|_{x=x_0} = f(x_0, t_0) \tag{2.11}$$

Therefore

$$\Delta x = \left.\frac{dx}{dt}\right|_{x=x_0} . \Delta t \tag{2.12}$$

The value of *x* at $t = t_0$+Δt is given by

$$x_1 = x_0 + \Delta x = x_0 + \left.\frac{dx}{dt}\right|_{x=x_0} . \Delta t \tag{2.13}$$

The Euler method is equivalent to using the first two terms of the taylor series expansion for *x* around the point (x_0, t_0):

$$x_1 = x_0 + \Delta t(\dot{x_0}) + \frac{\Delta t^2}{2!}(\ddot{x_0}) + \frac{\Delta t^3}{3!}\dddot{x_0} + \cdots \tag{2.14}$$

After using the Euler technique for determining *x*=x_1 corresponding to *t*=t_1 we can take another short time step Δt and determine x_2 corresponding to $t_2 = t_1 + \Delta t$ as follows:

$$x_2 = x_1 + \left.\frac{dx}{dt}\right|_{x=x_1} . \Delta t \tag{2.15}$$

By applying this the technique successively, values of *x* can be determined corresponding to different values of *t*. This method considers only the first derivative of *x* and is, therefore referred to as a first-order method. To give sufficient accuracy for each step, Δt has to be small. This will increase round-off errors, and the computational effort required will be high.

2.3.2. Modified Euler's Method of Integration

The standard Euler method results in inaccuracies because it uses the derivative at the beginning of the interval as though it applied throughout the interval. The modified Euler method tries to overcome this problem by using the average of the derivatives at the two ends.

The modified Euler method consists of the following steps:

Predictor Step: By using the derivative at the beginning of the step, the value at the end of the step is predicted

$$x_1^{(p)} = x_0 + \left.\frac{dx}{dt}\right|_{x=x_0} . \Delta t \tag{2.16}$$

Corrector Step: By using the predicted value of $x_1^{(p)}$, the derivative at the end of the step is computed and the average of this derivative and the derivative at the beginning of the step is used to find the corrected value

With the calculated value of $y_1^{(1)}$, calculate the approximate value of $\frac{dy}{dx}$ at $x = x_0$

$$x_1^{(c)} = x_0 + \frac{1}{2}\left(\left.\frac{dx}{dt}\right|_{x=x_0} + \left.\frac{dx}{dt}\right|_{x=x_0 p}\right)\Delta t \tag{2.17}$$

If desired, a more accurate value of the derivative at the end of the step can be calculated, again by using $x = x_1^{(c)}$. This derivative can be used to calculate a more accurate value of the average derivative which is in turn used to apply the corrector step again. This process can be used repeatedly until successive steps converge with desired accuracy. The modified Euler method is the simplest of predictor- corrector (P-C) methods.

2.3.3. Runga Kutta (R-K) Methods

The R-K methods approximate the Taylor series solution; however unlike the formal Taylor series solution, the R-K methods do not require explicit evaluation of derivatives higher than the first. The effects of higher derivatives are included by several evaluations of the first derivative. Depending on the number of terms effectively retained in the Taylor series, we have R-K methods of different orders.

Second-order R-K method

Referring to the differential equation in 2.10, the second-order R-K formula for the value of *x* at $t = t_0 + \Delta t$ is

$$x_1 = x_0 + \Delta x = x_0 + \frac{k_1 + k_2}{2} \tag{2.18}$$

Where

$$k_1 = f(x_0, t_0)\Delta t \tag{2.19}$$

$$k_2 = f(x_0 + k_1, t_0 + \Delta t)\Delta t \tag{2.20}$$

This method is equivalent to considering first and second derivative terms in the Taylor series; error is on the order of Δt^3. A general formula giving the value of *x* for the $(n+1)^{st}$ step is

$$x_{n+1} = x_n + \frac{k_1 + k_2}{2} \tag{2.21}$$

Where

$$k_1 = f(x_n, t_n)\Delta t \tag{2.22}$$

$$k_2 = f(x_n + k_1, t_n + \Delta t)\Delta t \tag{2.23}$$

Fourth-order R-K method

The general formula giving the value of *x* for the $(n+1)^{st}$ step is

$$x_{n+1} = x_0 + \frac{1}{6}(k_1 + 2k_2 + 2k_3 + k_4) \tag{2.24}$$

In equation (2.24)

$$k_1 = f(x_n, y_n)\Delta t \tag{2.25}$$

$$k_2 = f\left(x_n + \frac{k_1}{2}, t_n + \frac{\Delta t}{2}\right)\Delta t \tag{2.26}$$

$$k_3 = f\left(x_n + \frac{k_2}{2}, t_n + \frac{\Delta t}{2}\right)\Delta t \tag{2.27}$$

$$k_4 = f(x_n + k_3, t_0 + \Delta t)\Delta t \tag{2.28}$$

The physical interpretation of the above solution is as follows:

k_1 = (slope at the beginning of the time step) Δt

k_2 = (first approximation to slope at midstep) Δt

k_3 = (second approximation to slope at midstep) Δt

k_4 = (slope at the end of step) Δt

Δx = 1/6($k_1 + 2\,k_2 + 2\,k_3 + \,k_4$)

Thus Δx is the incremental value of *x* given by the weighted average of estimates based on slopes at the beginning, midpoint, and end of the time step.

2.4. Direct Methods for Transient Stability Analysis

The direct methods determine stability without explicitly solving the system differential equations. This approach has received considerable attention since the early work of

Magnusson [10] and Aylett [11] who used transient energy function for stability assessment. The transient energy approach can be described by considering a ball rolling on the inner surface of a bowl generated by the equation describing the transient energy of the system as depicted in Figure 2.9. The area inside the bowl represents the region of stability and the area outside represents the region of instability. The rim of the bowl represents maximum elevation to δ^s, and hence, maximum potential energy for the traversed trajectory caused by the fault energy.

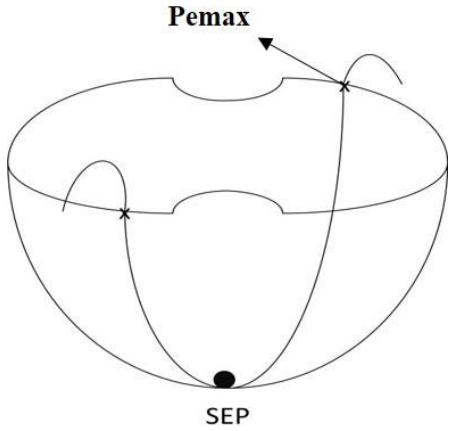

FIGURE 2.4: A ball rolling on the inner surface of a bowl [7].

Initially, the ball is at rest at the bottom of the bowl, and this state is referred to as the stable equilibrium point (SEP). When the bowl is perturbed, some kinetic energy is injected into the ball causing it to move from its location at SEP in a particular direction. The ball will roll up the inside surface of the bowl along a path determined by the direction of initial motion, and the point where the ball will stop is determined by the amount of the initially injected kinetic energy. If the ball converts all its kinetic energy into potential energy before reaching the rim, then it will roll back and eventually settle down at the stable equilibrium point again. However, if the injected kinetic energy is high enough to cause the ball to go over

the rim, then the ball will enter the region of instability and will not return to the SEP. The surface inside the bowl represents the potential energy surface and the rim of the bowl represents the potential energy boundary surface (PEBS.)The application of transient energy function (TEF) method to power systems is conceptually similar to that of a rolling ball in a bowl in the hyperspace (n-dimensional space). Initially, the system is operating at steady-state equilibrium point. If a fault occurs, the equilibrium is disturbed causing the synchronous machines to accelerate. The power system gains kinetic energy and potential energy during the fault-on period causing the system to move away from the SEP. After clearing the fault, the kinetic energy is converted to potential energy. For a system to avoid instability, the system must be capable of absorbing the kinetic energy at a time when the forces on the generators tend to bring them toward new equilibrium positions. For a given post-disturbance network configuration, there is a maximum or critical amount of transient energy that the system can absorb. Direct methods are suitable for on-line operation for dynamic security assessment because it only requires simple mathematical operations unlike numerical methods which involve solving differential equations numerically. Direct methods may require solving the differential equation up to the point where the fault is cleared [7]

2.5. Summary

In this chapter, the concept of equal area criterion and numerical integration methods like Euler's methods, Modified Euler's method and Runga kutta methods of integration are explained in detail. After that, a short review of direct methods for transient stability studies and its application are discussed.

In the next chapter, various synchronous machine models for stability studies are discussed. These models include classical model, detailed model and multi machine models. Also, simulations are performed on WSCC (3 machine 9 bus test system) and simulation results are analyzed in detail.

CHAPTER 3 : SYNCHRONOUS MACHINE MODELS FOR STABILITY STUDIES

This chapter presents synchronous machine models available for stability analysis. Section 3.1 Section 3.2 Section 3.3 present overview of machine models. Synchronous reference frame and center of inertia reference frame are presented in Section 3.4 Section 3.5. Multi-machine models, test system and simulation results are presented in Section 3.6 Section 3.7. Section 3.8 presents summary of the chapter.

3.1. Overview

A synchronous machine is one of the most important power system components. It can generate active and reactive power independently and has an important role in voltage control. The synchronizing torques between generators act to keep large power systems together and make all generator rotors rotate synchronously. This rotational speed is what determines the mains frequency which is kept very close to the nominal value of 50 or 60 Hz [12]. Generally, the well-established Park's model for a synchronous machine is used in system analysis. However, some modifications can be employed to simplify it for stability analysis. Depending on the nature of the study, several models of a synchronous generator, having different levels of complexity, can be utilized [1]. In the simplest case, a synchronous generator is represented by a second-order differential equation, while studying fast transients in a generator's windings requires the use of a more detailed model, e.g., a sub-transient 6th-order model.

3.2. Classical Model

This is the "simplest" model used in stability studies. It is usually limited to analysis of first swing transients. The assumptions commonly made are [13].

a) Mechanical power input is constant

b) Damping or asynchronous power is neglected

c) The generator is represented by a constant EMF behind the direct axis transient reactance

d) The mechanical rotor angle of a synchronous generator can be represented by the angle of the voltage behind transient reactance

Consider the single-machine infinite-bus (SMIB) system shown in Figure 3.1

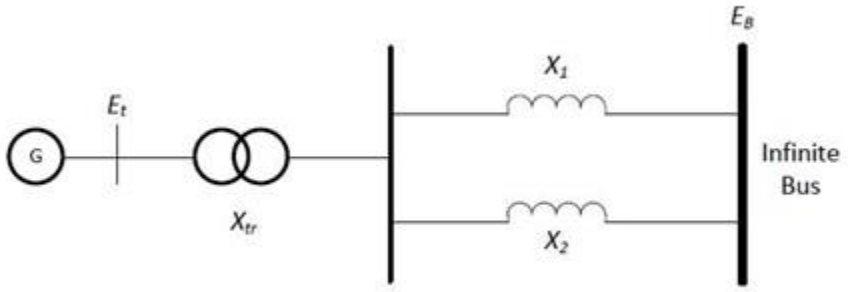

FIGURE 3.1: Single-machine infinite-bus system [1]

The generator is represented by the classical model, which ignores saliency of round rotor, that is, for the purpose of transient stability, only the transient reactance $X'_d$is considered with the assumption that the direct and quadrature components are equal. Also, the speed governor effects are neglected. The generator's voltage is denoted by *E'*, and the infinite-bus voltage is denoted by E_B. The rotor angle δ represents the angle by which *E'* leads E_B. When the system experiences a disturbance, the magnitude of *E'* remains constant at its

pre-disturbance value and δ changes as the generator rotor speed deviates from synchronous speed w_0.

The generator's electrical power output is

$$P_e = \frac{E'E_s}{X_T} sin\delta = P_{max} sin\delta \quad (3.1)$$

Where $$P_{max} = \frac{E'E_s}{X_T} \quad (3.2)$$

Swing equation may be written as

$$\frac{2H}{w_0}\frac{d^2\delta}{dt^2} = P_m - P_{max} sin\delta \quad (3.3)$$

Where

P_m = mechanical power input, in pu

P_{max} = maximum electrical power output, in pu

H = inertia constant, in MW.s/MVA

δ = rotor angle, in elec. rad

t = time, in s

3.3. Detailed Model

In this model of synchronous machine, the field coil on the direct axis (d-axis) and damper coil on the quadrature axis (q-axis) are considered. The machine differential equations are [14].

$$\frac{dE'_q}{dt} = \frac{1}{T'_{do}}\left[-E'_q + (X_d - X'_d)i_d + E_{fd}\right] \quad (3.4)$$

$$\frac{dE'_d}{dt} = \frac{1}{T'_{qo}}\left[-E'_d + \left(X_q - X'_q\right)i_q\right] \quad (3.5)$$

$$\frac{d\delta}{dt} = w_B(S_m - S_{m0}) \quad (3.6)$$

$$\frac{dS_m}{dt} = \frac{1}{2H}[T_m - DS_m - T_e] \tag{3.7}$$

$$T_e = E'_q i_q + E'_d i_d + \left(X_q - X'_q\right) i_d i_q \tag{3.8}$$

$$E'_q + X'_d i_d - R_a i_q = v_q \tag{3.9}$$

$$E'_d + X'_q i_q - R_a i_d = v_d \tag{3.10}$$

From Equations (3.9) and (3.10), i_d and i_q can be solved as

$$\begin{bmatrix} i_q \\ i_d \end{bmatrix} = \frac{1}{R_a^2 + X'_d X'_q} \begin{bmatrix} R_a & X'_d \\ -X'_q & R_a \end{bmatrix} \begin{bmatrix} E'_q & -v_q \\ E'_d & -v_d \end{bmatrix} \tag{3.11}$$

Where

T_m = the mechanical torque in the direction of rotation

T_e = the electrical torque opposing the mechanical torque

T'_{do} = d-axis open circuit transient time constant

T'_{qo} = q-axis open circuit transient time constant

S_m = machine slip

S_{m0} = initial machine slip (= *0* in steady-state)

w_B = the electrical angular frequency

X_d= d-axis reactance

X_q= q-axis reactance

X'_d, X'_q = d-axis and q-axis transient reactance, respectively

R_a = armature resistance

E'_d, E'_q = d-axis and q-axis generator's voltage

i_d, i_q = d-axis and q-axis current

E_{fd} = control voltage

3.4. Synchronous Reference Frame

The set of differential equations for synchronous reference frame are

$$M_i \dot{w}_\iota + D_i w_i = P_{mi} - P_{ei} \tag{3.12}$$

$$\dot{\delta}_\iota = w_i \qquad i = 1,2,3, \ldots . n \tag{3.13}$$

Where, for machine *i*,

δ_i= angle of voltage behind transient reactance, indicative of generator rotor position

w_i= rotor speed

M_i= generator inertia constant

D_i= damping coefficient

3.5. Center Of Inertia Reference Frame (COI)

The center of inertia model gives a good physical insight into the behavior of synchronous generators. The equation of motion of the generators in the COI reference frame can be represented by [15].

$$M_i \dot{\widetilde{w}_\iota} = P_{mi} - P_{ei} - \frac{M_i}{M_T} P_{coi} - D_i \widetilde{w_\iota} \tag{3.14}$$

$$\dot{\theta}_\iota = \widetilde{w_\iota} \qquad i = 1,2,3, \ldots . n \tag{3.15}$$

The angle displacement $\dot{\theta}_\iota$ and angular velocity $\widetilde{w_\iota}$ are defined as

$$\theta_i = \delta_i - \delta_0 \tag{3.16}$$

$$\widetilde{w_\iota} = \dot{\theta}_\iota = w_i - w_0 \tag{3.17}$$

Where

$$M_T = \sum_{i=1}^{n} M_i \tag{3.18}$$

$$\delta_0 = \frac{1}{M_T} \sum_{i=1}^{n} M_i \, \delta_i \tag{3.19}$$

$$w_0 = \frac{1}{M_T} \sum_{i=1}^{n} M_i \, w_i \tag{3.20}$$

$$P_{coi} = \sum_{i=1}^{n}(P_{mi} - P_{ei}) \quad (3.21)$$

3.6. Multi Machine Models for Transient Stability

Multi machine equations can be written similar to the one-machine system connected to the infinite bus. In order to reduce the complexity of the transient stability analysis, similar simplifying assumptions are made as follows [6].

a) Each synchronous machine is represented by a constant voltage source behind the direct axis transient reactance. This representation neglects the effect of the saliency and assumes constant flux linkages.

b) The governor's actions are neglected and the input powers are assumed to remain constant during the entire period of simulation.

c) Using the prefault bus voltages, all loads are converted to equivalent admittances to ground and are assumed to remain constant.

d) Damping or asynchronous powers are ignored.

e) The mechanical rotor angle of each machine coincides with the angle of the voltage behind the machine reactance.

f) Machines belonging to the same station swing together and are said to be coherent. A group of coherent machines is represented by one equivalent machine.

The first step in the transient stability analysis is to solve the initial load flow and to determine the initial bus voltage magnitudes and phase angles. The machine currents prior to disturbance are calculated from

$$I_i = \frac{S_i^*}{V_i^*} = \frac{P_i - jQ_i}{V_i^*} \qquad i = 1,2,3, \ldots \ldots, m \quad (3.22)$$

Where m is the number of generators. V_i is the terminal voltage of the ith generator. P_i and Q_i are the generator real and reactive power. All unknown values

are determined from the initial power flow solution. The generator armature resistances are usually neglected and the voltage behind the transient reactances are obtained.

$$E_i' = V_i + jX_d' I_i \tag{3.23}$$

Next all loads are converted to equivalent admittances by using the relation

$$y_{i0} = \frac{S_i^*}{|V_i|\text{^}2} = \frac{P_i - jQ_i}{|V_i|\text{^}2} \tag{3.24}$$

To include voltage behind transient reactances, *m* buses are added to the *n*-bus power system network. The equivalent network with all loads converted to admittances is shown in figure 3.4.

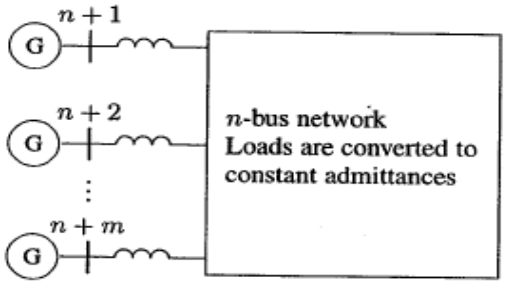

FIGURE 3.2: Power system representation for transient stability analysis. [6].

Nodes *n*+1, *n*+2,……, *n*+*m* are the internal machine buses, i.e., the buses behind the transient reactances. The node voltage equation with node 0 as reference for this network

$$\begin{bmatrix} I_1 \\ \vdots \\ I_n \\ \hline I_{n+1} \\ \vdots \\ I_{n+m} \end{bmatrix} = \begin{bmatrix} Y_{11} & \cdots & Y_{1n} & Y_{1(n+1)} & \cdots & Y_{1(n+m)} \\ \vdots & \ddots & \vdots & \vdots & \ddots & \vdots \\ Y_{n1} & \cdots & Y_{nn} & Y_{n(n+1)} & \cdots & Y_{n(n+m)} \\ \hline Y_{(n+1)1} & \cdots & Y_{(n+1)n} & Y_{(n+1)(n+1)} & \cdots & Y_{(n+1)(n+m)} \\ \vdots & \ddots & \vdots & \vdots & \ddots & \vdots \\ Y_{(n+m)1} & \cdots & Y_{(n+m)n} & Y_{(n+m)(n+1)} & \cdots & Y_{(n+m)(n+m)} \end{bmatrix} \begin{bmatrix} V_1 \\ \vdots \\ V_n \\ \hline E'_{n+1} \\ \vdots \\ E'_{n+m} \end{bmatrix} \tag{3.25}$$

$$I_{bus} = Y_{bus} V_{bus} \tag{3.26}$$

Where I_{bus} is the vector of the injected bus currents and V_{bus} is the vector of bus voltages measured from the reference node. The diagonal elements of the bus admittance matrix are the sum of admittances connected to it, and the off-diagonal elements are equal to the negative of the admittances between the nodes.

To simplify the analysis, all nodes other than the generator nodes are eliminated using the Kron reduction formula. To eliminate the load buses, the bus admittance matrix in (3.25) is partitioned such that the *n* buses to be removed are represented in the upper *n* rows. Since no current enters or leaves the load buses, currents in the *n* rows are zero. The generator currents are denoted by the vector I_m and the generator and load voltages are represented by the vectors E'_m and V_n, respectively. Then, equation (3.25), in terms of submatrices, becomes

$$\begin{bmatrix} 0 \\ I_m \end{bmatrix} = \begin{bmatrix} Y_{nn} & Y_{nm} \\ Y_{nm}^t & Y_{mm} \end{bmatrix} \begin{bmatrix} V_n \\ E'_m \end{bmatrix} \tag{3.27}$$

The voltage vector V_n may be eliminated by the substitution as follows.

$$0 = Y_{nn}V_n + Y_{nm}E'_m \tag{3.28}$$

$$I_m = Y_{nm}^t V_n + Y_{mm}E'_m \tag{3.29}$$

From equation (3.28)

$$V_n = -Y_{nn}^{-1}Y_{nm}E'_m \tag{3.30}$$

Now substituting into equation (3.29) we have

$$I_m = [Y_{mm} - Y_{nm}^t Y_{nn}^{-1} Y_{nm}]E'_m \tag{3.31}$$

$$I_m = Y_{bus}^{red} E'_m \tag{3.32}$$

$$Y_{bus}^{red} = [Y_{mm} - Y_{nm}^t Y_{nn}^{-1} Y_{nm}] \tag{3.33}$$

The reduced bus admittance matrix has the dimensions (m*m), where *m* is the number of generators. The electrical power output of each machine can now be expressed in terms of the machine's internal voltage.

$$P_{ei} = \sum_{j=1}^{m} |E_i'| \left| E_j' \right| \left| Y_{ij} \right| \cos\left(\theta_{ij} - \delta_i + \delta_j\right) \tag{3.34}$$

Prior to disturbance, there is equilibrium between the mechanical power input and the electrical power output, and we have

$$P_{mi} = \sum_{j=1}^{m} |E_i'| \left| E_j' \right| \left| Y_{ij} \right| \cos\left(\theta_{ij} - \delta_i + \delta_j\right) \tag{3.35}$$

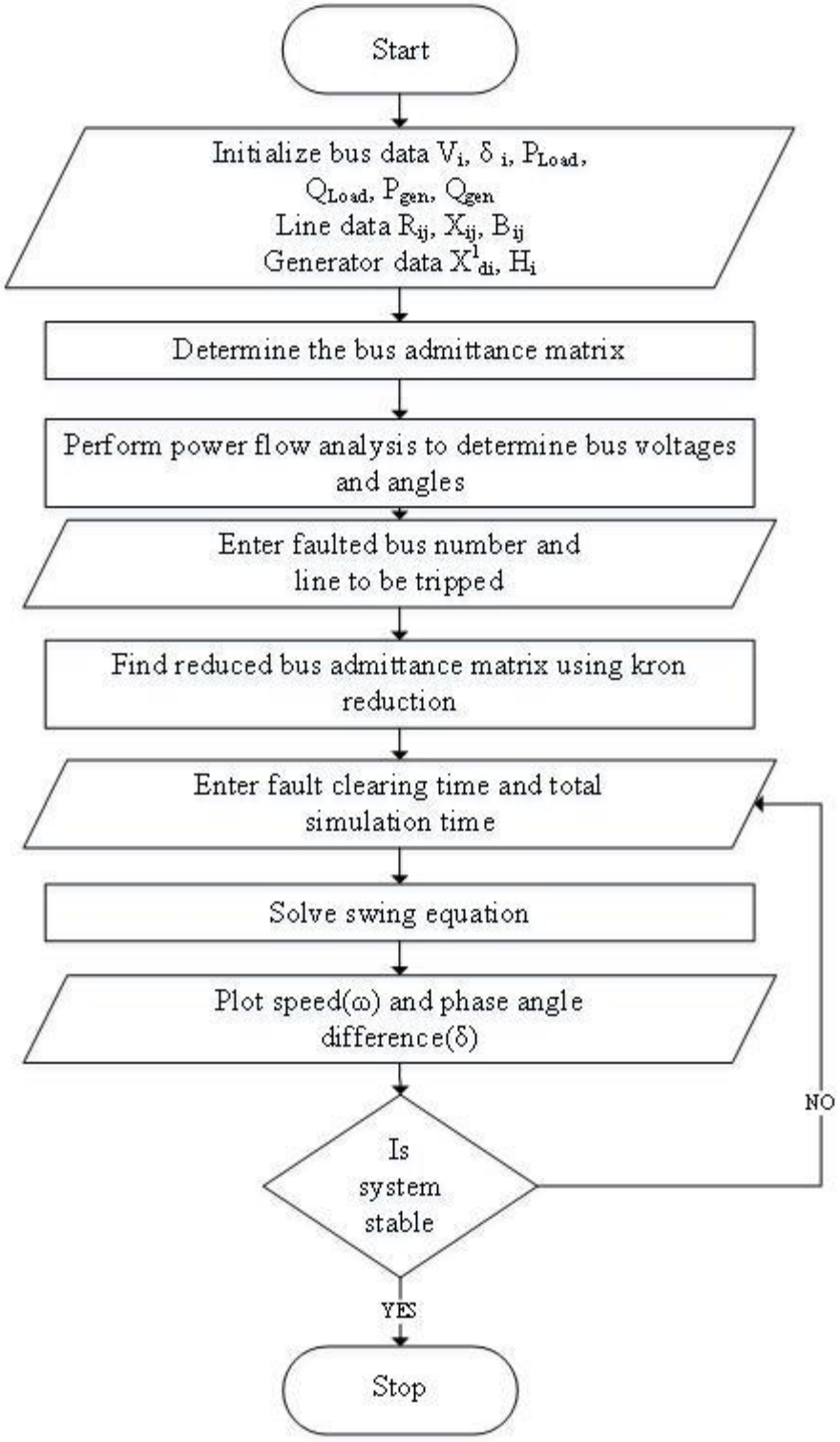

FIGURE 3.3: Flow chart for multi machine transient stability

3.7. Test System

Transient stability analysis is done on WSCC 9-bus (IEEE 9 BUS) test system, Classical model of generators were used and loads were assumed to be constant impedance loads.

3.7.1. WSCC 9-Bus Test System

WSCC 9-bus test case represents a simple approximation of the Western System Coordinating Council (WSCC) to an equivalent system with nine buses and three generators. The base KV levels are 13.8 kV, 16.5 kV, 18 kV, and 230 kV. The line complex powers are around hundreds of MVA each. As a test case, the WSCC 9-bus case is easy to control, as it has few voltage control devices [16].

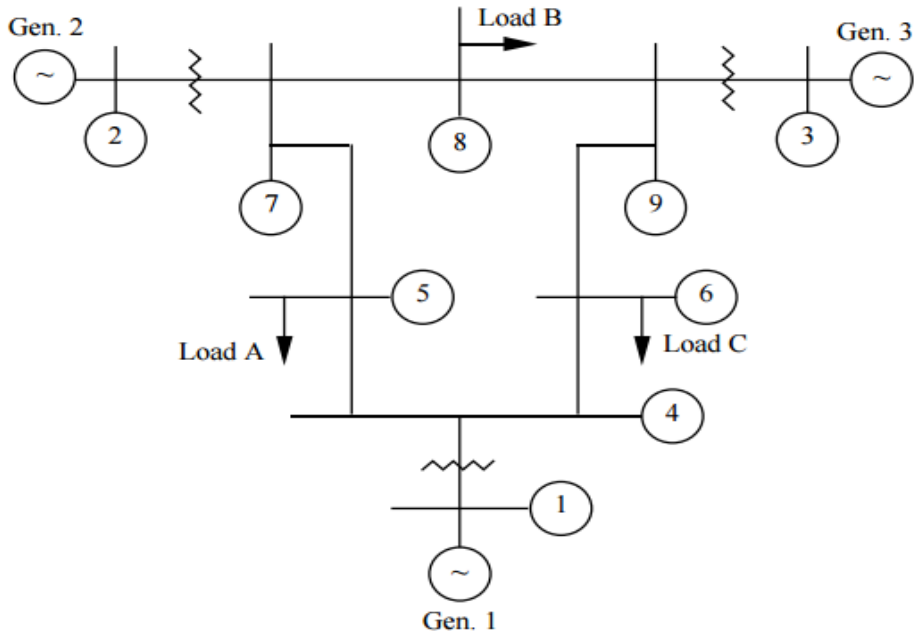

FIGURE 3.4: WSCC 9-bus test system

3.7.2. WSCC 9-Bus Test System Data [17]

Transmission line data:

TABLE 3.1: Transmission line data

Line	Resistance (PU)	Reactance(PU)	Half line charging (PU)
1 to 4	0	0.0576	0
2 to 7	0	0.0625	0
3 to 9	0	0.0586	0
4 to 5	0.010	0.085	0.088
4 to 6	0.017	0.092	0.079
5 to 7	0.032	0.161	0.153
6 to 9	0.039	0.170	0.179
7 to 8	0.0085	0.072	0.0745
8 to 9	0.0119	0.1008	0.1045

Bus data:

TABLE 3.2: Bus Data

BUS NO.	BUS TYPE	GENERATION(PU)		LOAD(PU)		VOLTAGE MAGNITUDE (PU)
		P_G	Q_G	P_L	Q_L	
1	Swing	____	____	0.0	0.0	1.0400
2	PV	1.6300	____	0.0	0.0	1.0253
3	PV	0.8500	____	0.0	0.0	1.0253
4	PQ	0.0	0.0	0.0	0.0	_____
5	PQ	0.0	0.0	1.25	0.5	_____
6	PQ	0.0	0.0	0.9	0.3	_____
7	PQ	0.0	0.0	0.0	0.0	_____
8	PQ	0.0	0.0	1.0	0.35	_____
9	PQ	0.0	0.0	0.0	0.0	_____

Machine data:

TABLE 3.3: Machine Data

VARIABLE	MACHINE-1	MACHINE-2	MACHINE-3
X_d(PU)	0.1460	0.8958	1.3125
X'_d(PU)	0.0608	0.1198	0.1813
T'_{d0}(PU)	8.96	6.0	5.89
X_q(PU)	0.0969	0.8645	1.2578
X'_q(PU)	0.0608	0.1198	0.1813
T'_{q0}(PU)	0.3100	0.5350	0.6000
H(sec)	23.64	6.4	3.01
D(PU)	0.0254	0.0066	0.0026

3.7.3. Simulation Results

Case 1: A three phase bus fault is applied at bus 7 at 0.5 sec and fault is cleared at 0.6 sec.

Solid lines: No Damping.

Dashed lines: With Damping.

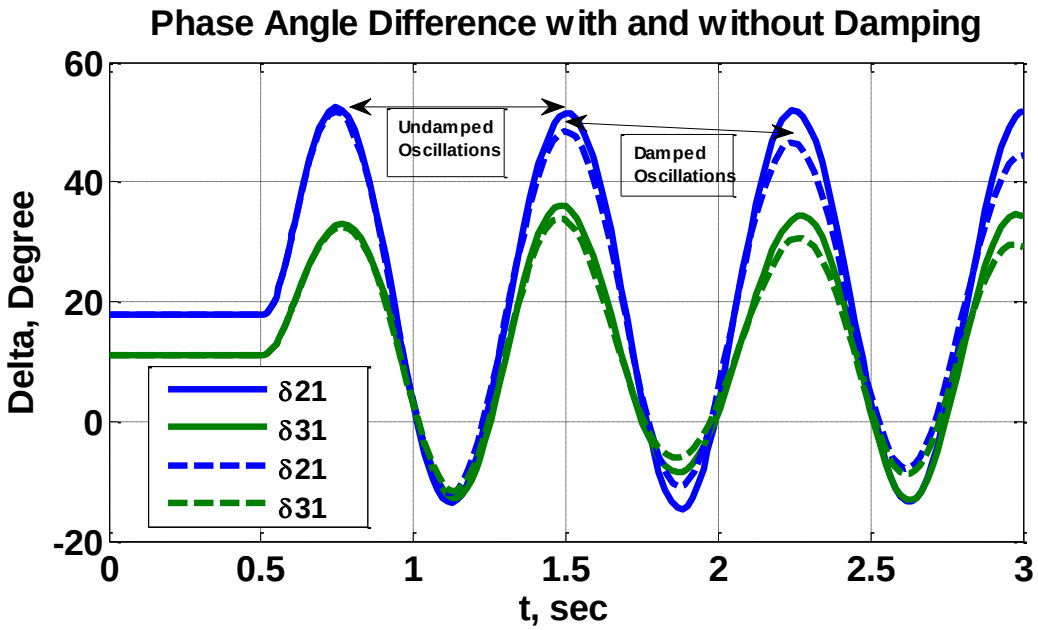

FIGURE 3.5: Plot for generator rotor angle versus time (tc= 0.6 sec). Solid lines represent plots without damping and dashed lines represent plots with damping.

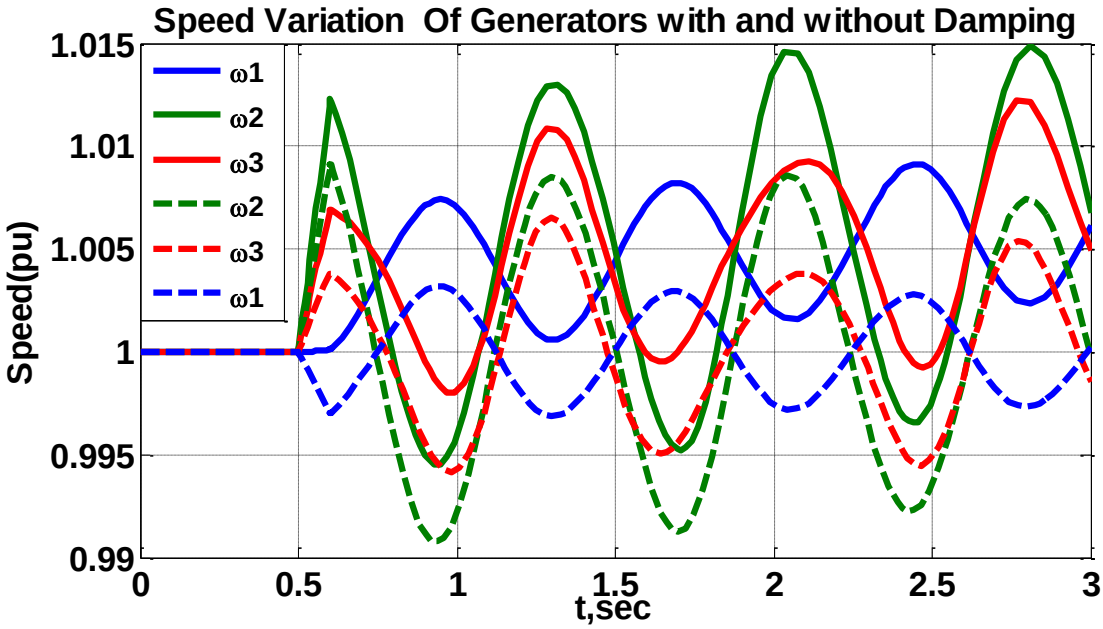

FIGURE 3.6: Plot for generator speed versus time (tc= 0.6 sec). Solid lines represent plots without damping and dashed lines represent plots with damping.

Case 2: A three phase bus fault is applied at bus 7 at 0.5 sec and fault is cleared at 0.73 sec.

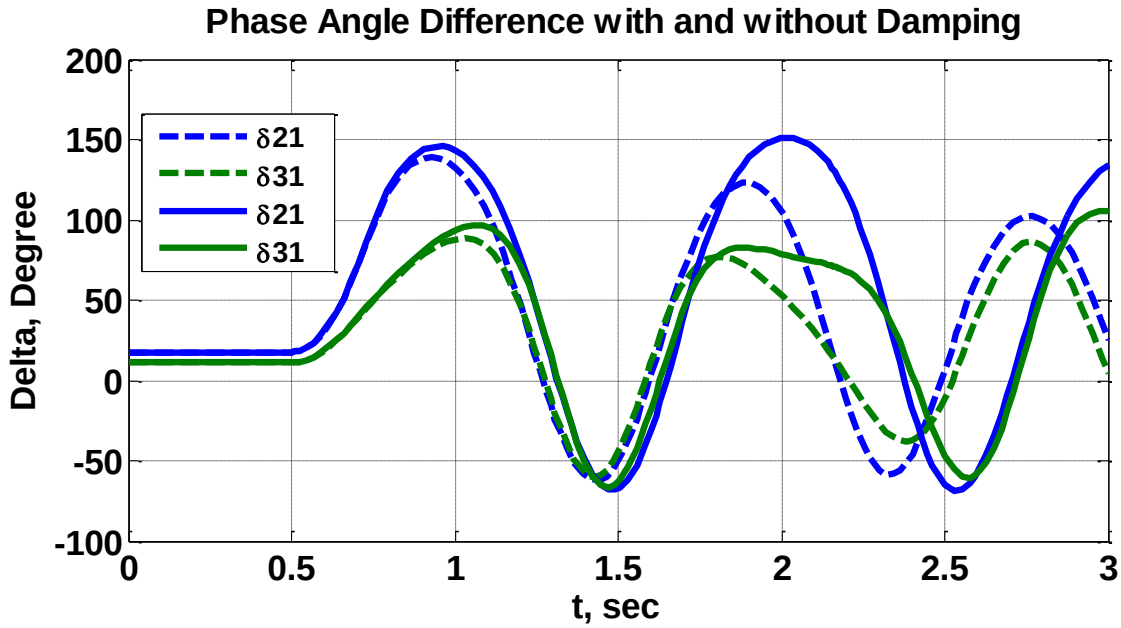

FIGURE 3.7: Plot for generator rotor angle versus time (tc= 0.73 sec). Solid lines represent plots without damping and dashed lines represent plots with damping.

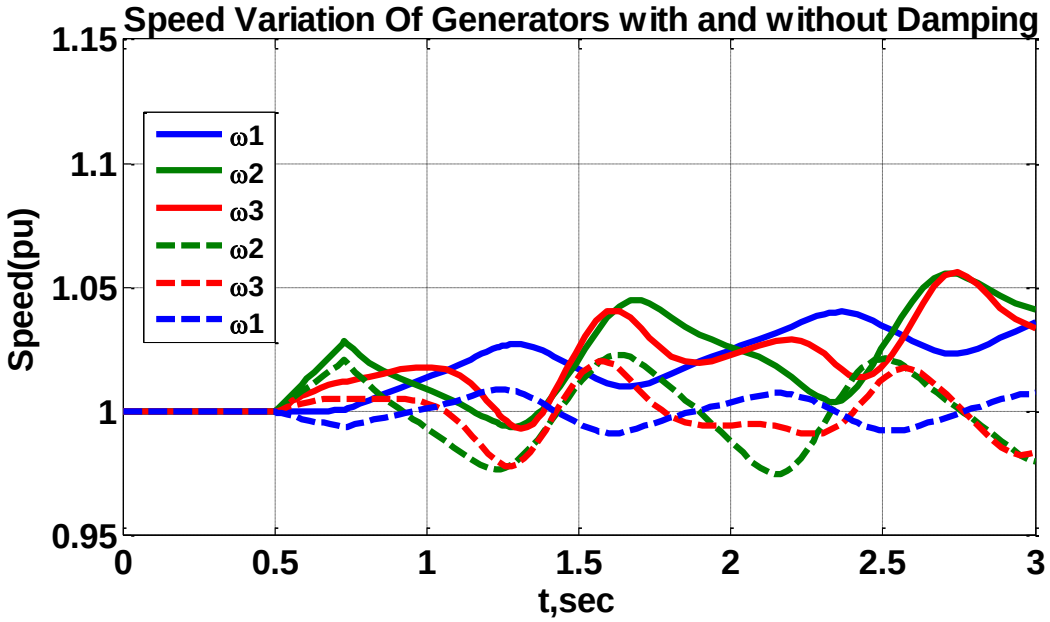

FIGURE 3.8: Plot for generator speed versus time (tc= 0.0.73 sec). Solid lines represent plots without damping and dashed lines represent plots with damping.

Case 3: A three phase bus fault is applied at bus 7 at 0.5 sec and fault is cleared at 0.74 sec.

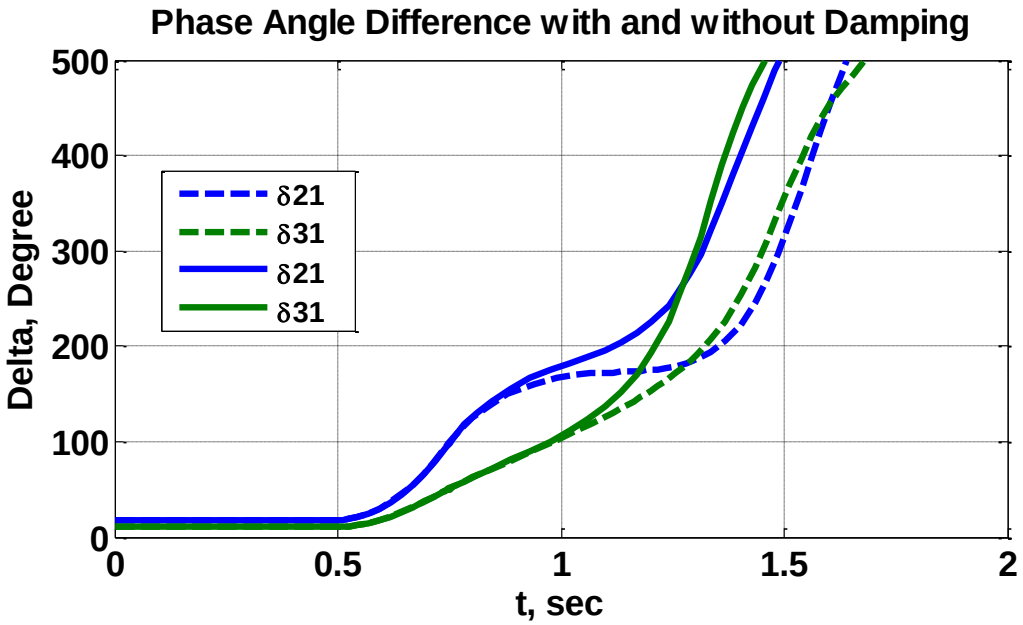

FIGURE 3.9: Plot for generator rotor angle versus time (tc= 0.74 sec). Solid lines represent plots without damping and dashed lines represent plots with damping.

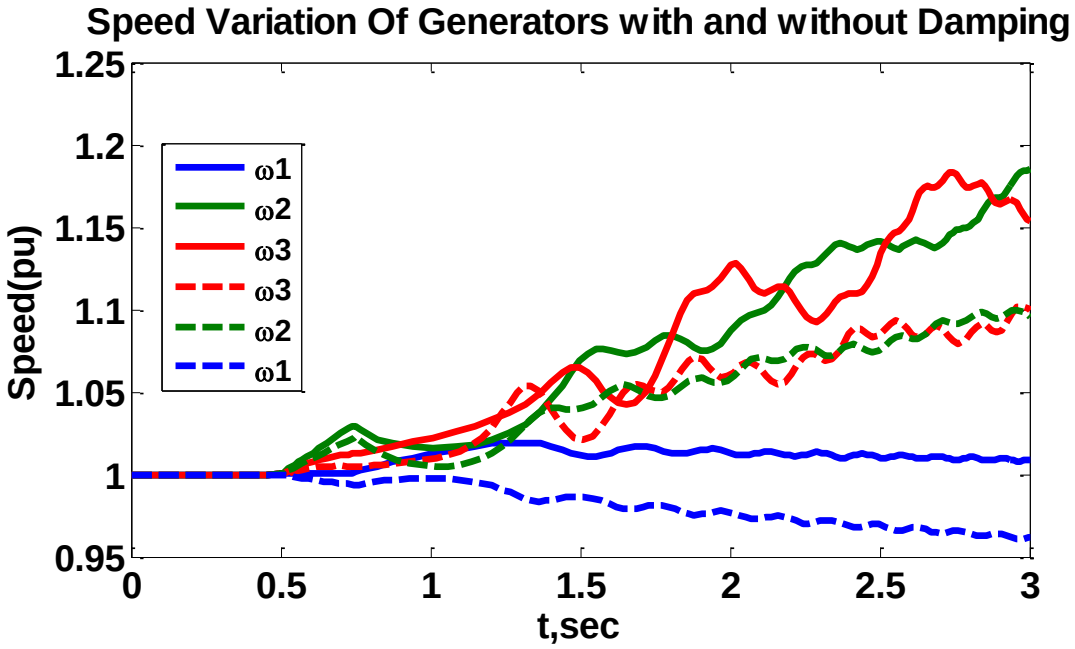

FIGURE 3.10: Plot for generator speed versus time (tc= 0.0.74 sec). Solid lines represent plots without damping and dashed lines represent plots with damping.

Case 4: A three phase fault is applied on line 5-7 close to bus 7 at 0.5 sec, and is cleared by the simultaneous opening of breakers at both ends of the line at 0.6 sec.

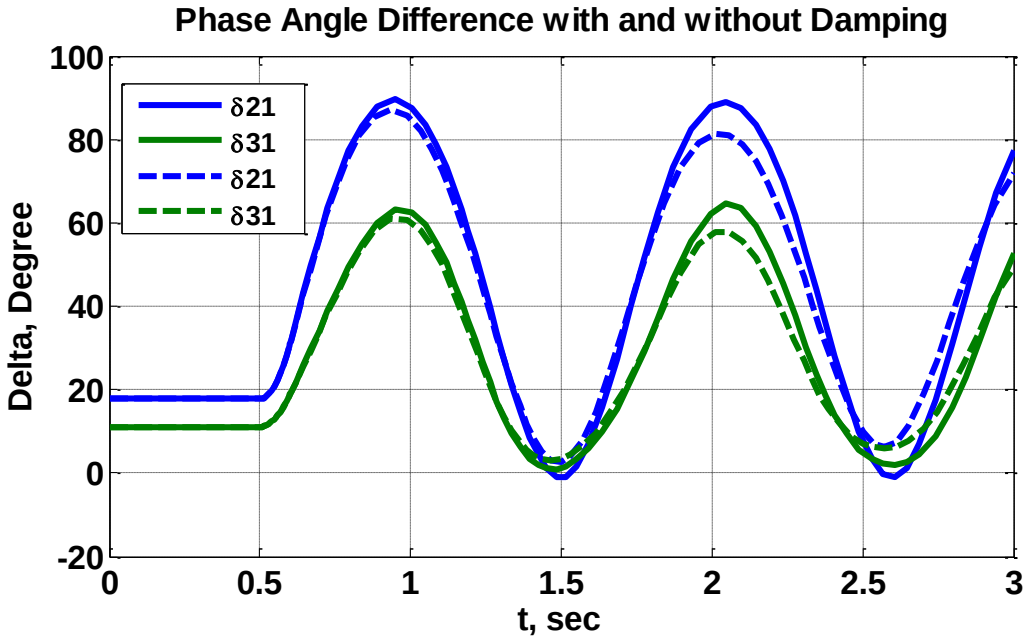

FIGURE 3.11: Plot for generator rotor angle versus time (tc= 0.6 sec, line 5-7 tripped). Solid lines represent plots without damping and dashed lines represent plots with damping.

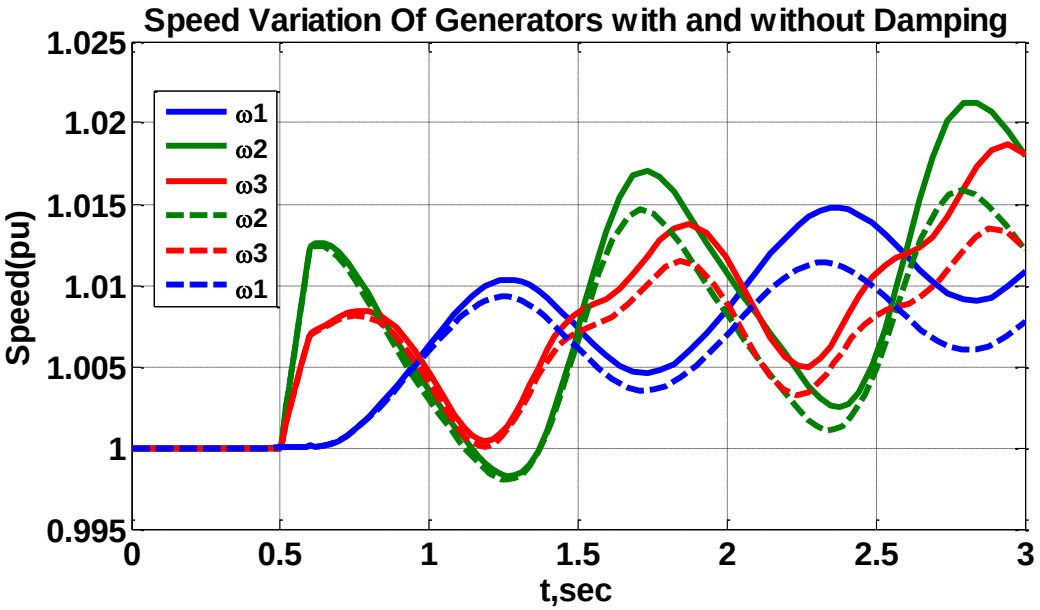

FIGURE 3.12: Plot for generator speed versus time (tc= 0.6 sec, line 5-7 tripped). Solid lines represent plots without damping and dashed lines represent plots with damping.

Case 5: A three phase fault is applied on line 5-7 close to bus 7 at 0.5 sec, and is cleared by the simultaneous opening of breakers at both ends of the line at 0.66 sec.

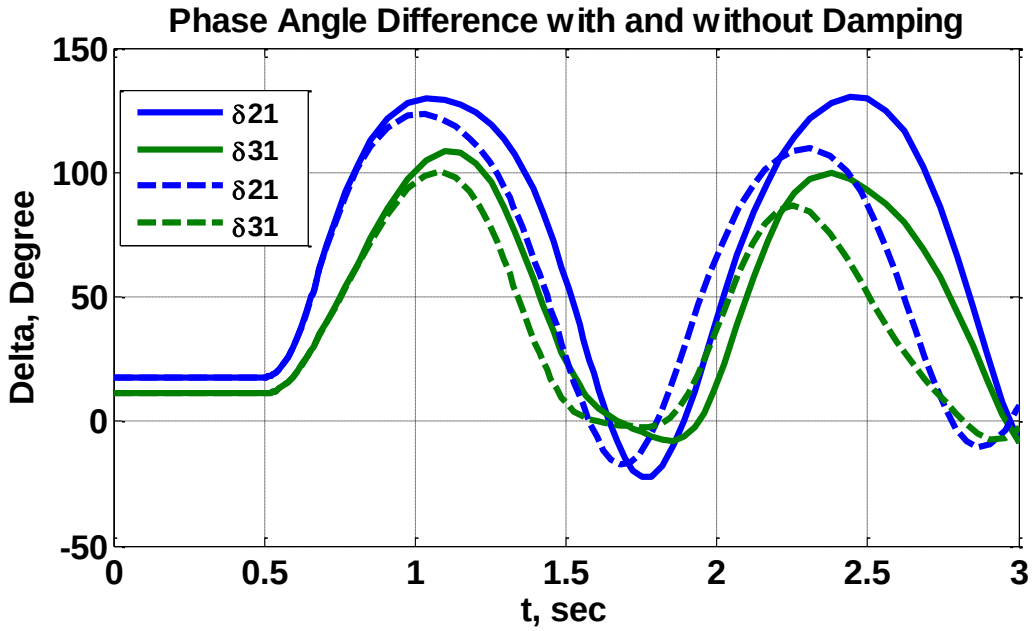

FIGURE 3.13: Plot for generator rotor angle versus time (tc= 0.66 sec, line 5-7 tripped). Solid lines represent plots without damping and dashed lines represent plots with damping.

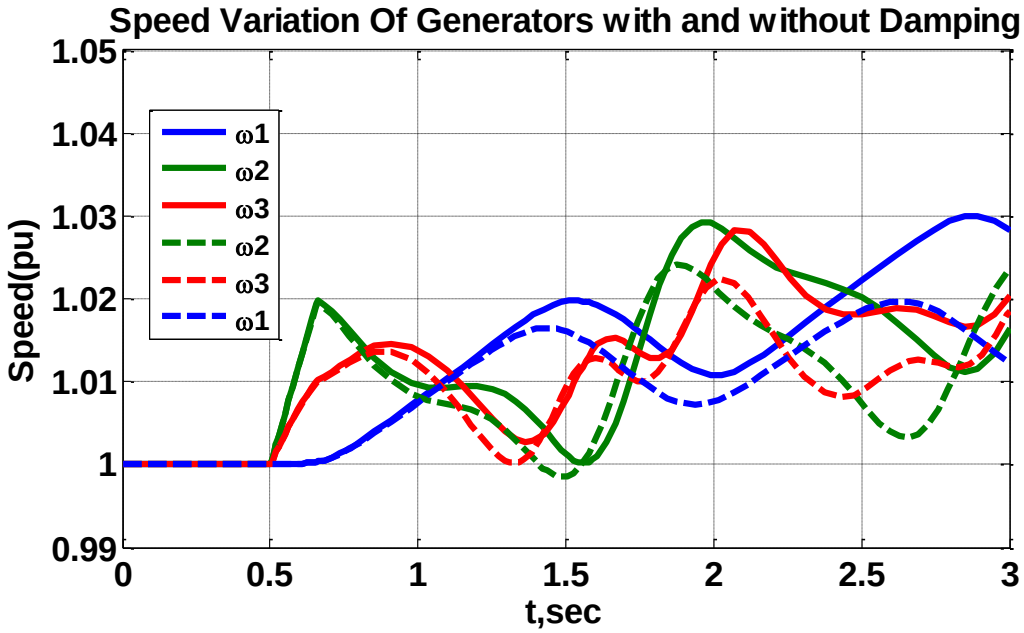

FIGURE 3.14: Plot for generator speed versus time (tc= 0.66 sec, line 5-7 tripped). Solid lines represent plots without damping and dashed lines represent plots with damping.

Case 6: A three phase fault is applied on line 5-7 close to bus 7 at 0.5 sec, and is cleared by the simultaneous opening of breakers at both ends of the line at 0.67 sec.

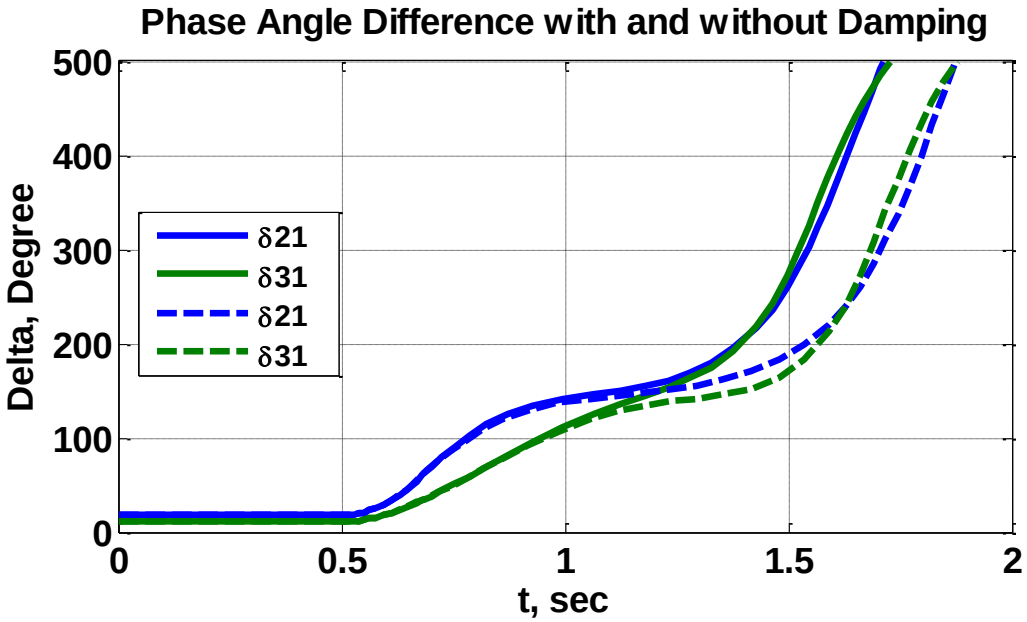

FIGURE 3.15: Plot for generator rotor angle versus time (tc= 0.67 sec, line 5-7 tripped). Solid lines represent plots without damping and dashed lines represent plots with damping.

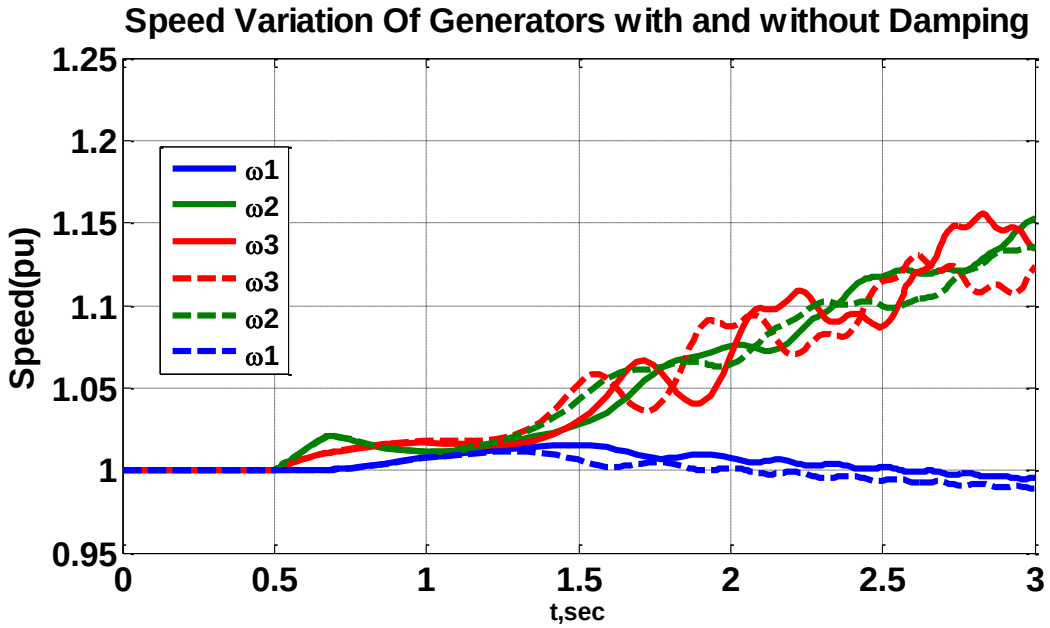

FIGURE 3.16: Plot for generator speed time (tc= 0.67 sec, line 5-7 tripped). Solid lines represent plots without damping and dashed lines represent plots with damping.

Case 7: Calculating critical clearing time for different fault locations

TABLE 3.4: Critical clearing time for different fault locations

Fault Type	Location	Line Removal By Breaker Opening	Critical Clearing Time(sec)
Three Phase fault	Bus 9	No	0.25
Three Phase fault	On Line 9,6 close to bus 9	Yes (9,6)	0.21
Three Phase fault	Bus 4	No	0.33
Three Phase fault	On Line 4,5 close to bus 4	Yes (4,5)	0.29
Three Phase fault	Bus 5	No	0.41
Three Phase fault	On Line 4,5 close to bus 5	Yes (4,5)	0.39
Three Phase fault	Bus 8	No	0.33
Three Phase fault	On Line 8,7 close to bus 8	Yes (8,7)	0.3

3.7.4. Simulation Results Analysis

Comprehensive transient stability analysis is done on WSCC 9-bus system by simulating three phase faults at different locations. This includes bus faults and line faults followed by removal of faulted lines. Key observations are

- For both three phase bus faults and line faults followed by line removal close to generator bus has smaller clearing time compared to the faults away from generating stations. This can be clearly observed from figures 3.7.3 to figures 3.7.14
- For a line fault close to a bus followed by removal of line creates more disturbance in the system than the bus fault where there is no line removal. Acceleration of generator angles more in this case, this can be observed form the figure 3.7.3 and figure 3.7.9. Moreover, critical clearing time is lesser for bus faults.
- Generator rotor angle oscillations are un-damped when damping is not considered and it takes more time for the system to settle to new equilibrium point. But with damping included, generator rotor angle oscillations are damped and settle to new

equilibrium point faster. The generator damping provides flux which will compensate the transient effect and machine tries to return back to synchronism, this can be observed from figure 3.7.3.

- Type of fault and location of fault has significant effect on the stability margin. Additionally, the faulted part must be isolated rapidly from the rest of the system to increase stability margin.

3.7.5. Transient Stability Analysis Using Center Of Inertia Reference Frame

Center of inertia model gives a good physical insight into the behavior of synchronous generator unlike synchronous reference frame because the reference angle δ_{coi} is time varying and all angles are measured with respect to this angle. So results based on center of inertia models are more accurate compared to synchronous reference frame. Moreover, use of coi reference frame leads to simpler expressions for transient energy functions as compared to synchronous reference frame, for this reason coi reference frame are often used in transient stability studies. Case 4 and Case 6 from 3.7.3 are simulated again but with center of inertia reference angle. And results are presented in figures 3.7.15, 3.7.16 and figures 3.7.17, 3.7.18, from which we can track the variation of all generator rotor angles and speed with respect to COI reference frame during a disturbance.

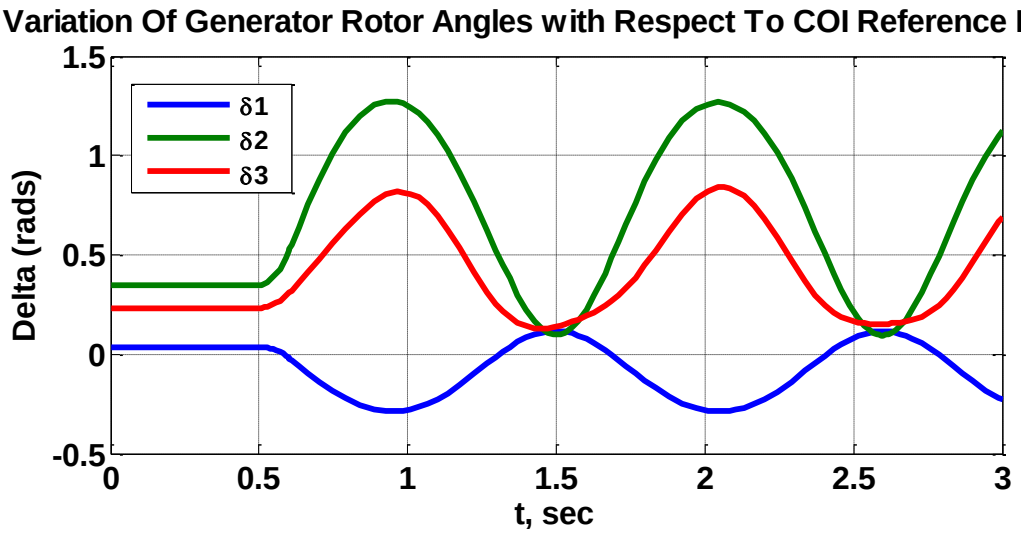

FIGURE 3.17: Plot for generator rotor angle versus time w.r.t COI reference frame (tc=0.6 sec)

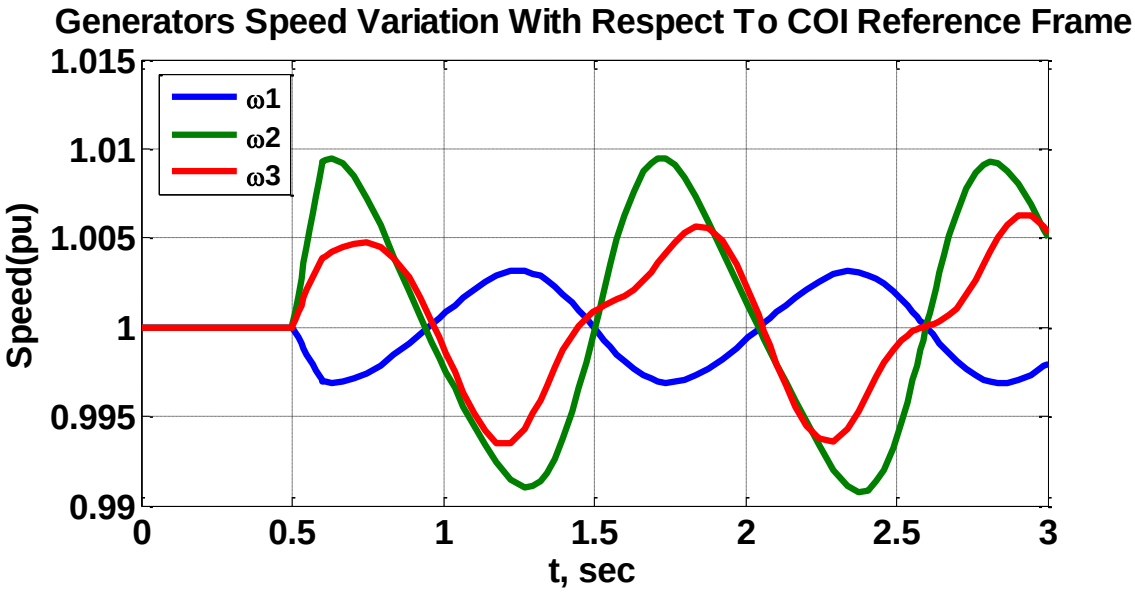

FIGURE 3.18: Plot for generator speed versus time w.r.t COI reference frame (tc=0.6 sec)

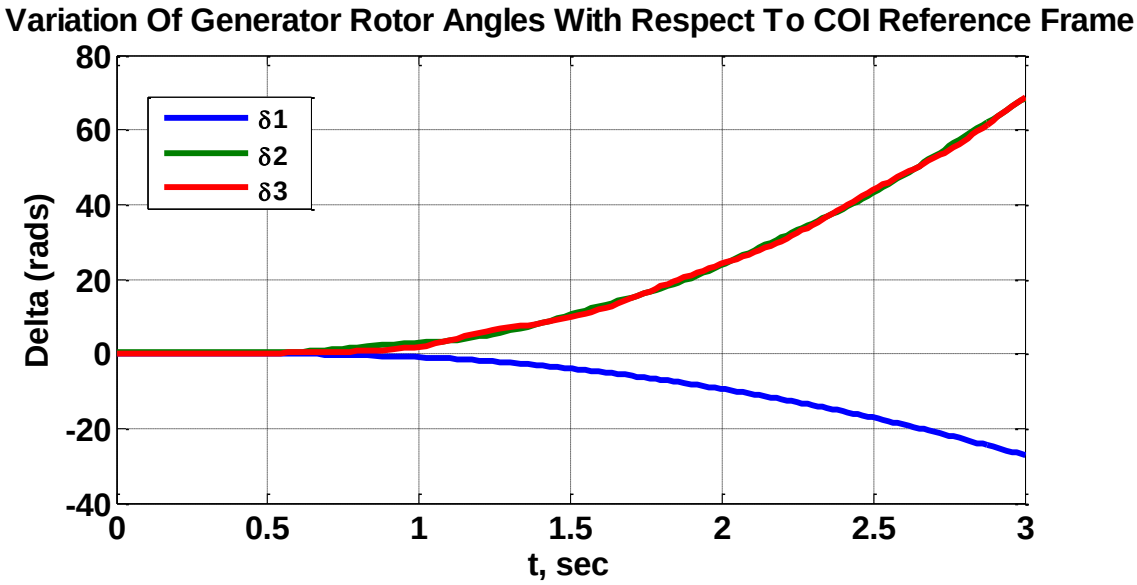

FIGURE 3.19: Plot for generator rotor angle versus time w.r.t COI reference frame (tc=0.67 sec)

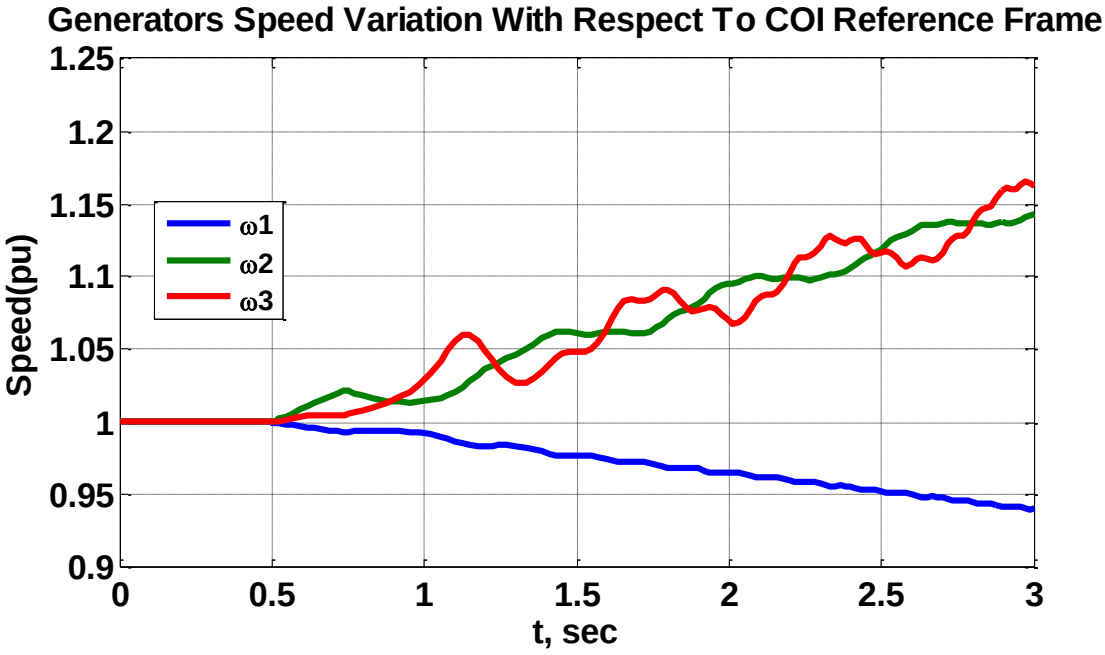

FIGURE 3.20: Plot for generator speed versus time w.r.t COI reference frame (tc=0.6 sec)

3.8. Summary

In this chapter, various synchronous machine models for stability studies are discussed. These models include classical model, detailed model and multi machine models. Also, swing equations for both synchronous reference frame and center of inertia reference frame are derived. Additionally, procedure for multi machine transient stability is presented and time domain analysis is done for both synchronous reference and COI reference frame for different location of fault on the test system.

In Chapter 4, concepts of direct methods and its applications for transient stability studies are explained in detail. Also, transient energy functions are discussed and transient stability analysis is done using direct methods.

CHAPTER 4 : TRANSIENT STABILITY STUDIES USING DIRECT METHODS

In this chapter transient stability analysis using direction methods and energy function formulation is presented. Section 4.1 Section 4.2 presents overview, theory and methodology of direct methods. Multi-machine transient stability analysis using direct methods and simulation results are presented in section 4.3. Summary of the chapter is presented in Section 4.4.

4.1. Overview

In transient stability, the critical clearing time of circuit breakers to clear a fault is the of vital importance when the system is subjected to large disturbances. In real-world application, the critical clearing time can be interpreted in terms of meaningful quantities such as maximum power transfer in the prefault state. The energy-based methods are a special case of the more general Lyapunov's second method or the direct method. The direct methods determine stability without explicitly solving the system differential equations. Energy function methods have proven to be good ways to determine transient stability in a more reliable way than numerical methods. Energy function methods are considered the future of dynamic security assessment [18].

4.2. Lyapunov's Method [18]

In 1892, A. M. Lyapunov proposed that stability of the equilibrium point of a nonlinear dynamic system of dimension *n* of:

$$\dot{x} = f(x), f(0) = 0 \tag{4.1}$$

can be ascertained without numerical integration. Lyapunov's theorem states that if there exists a scalar function *V(x)* for Equation 4.1 that is positive-definite around the equilibrium point "0" and the derivative $\dot{V}(x) < 0$, then the equilibrium is asymptotically stable. $\dot{V}(x)$ can be obtained as equation 4.2.

$$\dot{V}(x) = \nabla V^T . f(x) \tag{4.2}$$

V(x) is actually a generalization of the concept of the energy of a system. Application of the energy function method to power system stability began with the early work ofMagnusson [19] and Aylett [20]. Although many different Lyapunov functions have been tried since then, the first integral of motion, which is the sum of kinetic and potential energies, may have provided the best result. In power literature, Lyapunov's method has become the so-called Transient Energy Function (TEF) method.

4.3. Energy Function Theory and Methodology

4.3.1. Overview

As previously explained, the transient energy approach can be described by a ball rolling on the inner surface of a bowl as depicted in Figure 2.4. Initially the ball is resting which is equivalent to a power system in its steady-state equilibrium. When an external force is applied to the ball, the ball moves away from the equilibrium point. Equivalently, in a power system, a fault occurs on the system which causes the generator's rotors to accelerate and gain some kinetic energy causing the system to move away from the SEP. If the ball converts all its kinetic energy into potential energy before reaching the rim, then it will roll back and settle down at the SEP eventually. In power systems, after the fault is cleared, the kinetic energy gained during the fault will be converted into potential energy if the system

is capable enough to absorb that kinetic energy. Otherwise, the kinetic energy will increase causing the system's machines to lose synchronism and become unstable [7].

4.3.2. Mathematical Formulation

The sum of potential energy (PE) and kinetic energy (KE) for a conservative system is constant. The expression for total energy can be expressed in terms of KE and PE. Expression for the total energy of the system in terms of the state $= (\delta, \dot{\delta})$ [7]:

$$V(\delta) = \frac{1}{2} M \dot{\delta}^2 + \int_{\delta^0}^{\delta} P(u) du \tag{4.3}$$

When system is at equilibrium point (i.e., with $\delta = \delta^0$ and $\dot{\delta} = 0$), both the KE and PE are zero. Now, for the power system after time t $\geq T$, that is after the fault is cleared, the system energy is described by

$$V(\delta(t)) = \frac{1}{2} M \dot{\delta_T}^2 + \int_{\delta^0}^{\delta_T} P(u) du \tag{4.4}$$

Transient stability of the system can be predicted from the potential energy curve. In figure 4.1, the potential energy curve is illustrated.

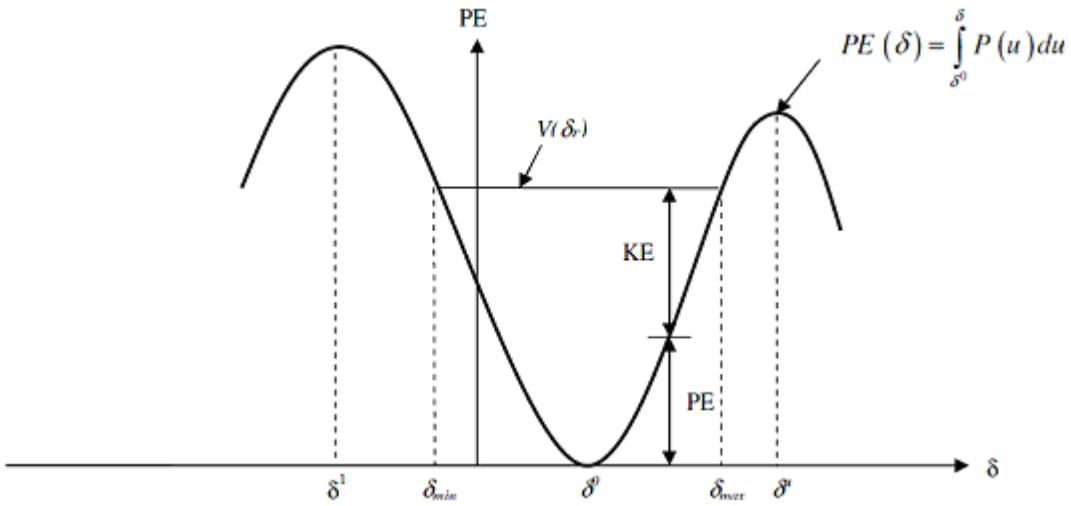

FIGURE 4.1: Potential energy plot. Redrawn from [7]

From the figure 4.1, the PE curve has a local minimum at $\delta = \delta^0$ and has two neighboring local maxima at δ^u and δ^l. Also, the plot shows that if the rotor angle reaches δ_{max}, the system becomes unstable, that is, if the fault is not cleared before the rotor angle becomes δ_{max}, the trajectory will diverge towards the UEP δ^u. For any T > $T_{critical}$, $\delta(\dot{t})$ is always positive and $\delta(t)$ increases monotonically with t.Assume the usual case of a SMIB system, with the generator delivering power [27].

From equation 4.3 and the definition of PE*max*, V(δ_T) < PE*max* implies that

$$\frac{1}{2}M\dot{\delta_T}^2 + \int_{\delta^0}^{\delta_T} P(u)du < \int_{\delta^0}^{\delta_u} P(u)du \tag{4.5}$$

The condition of stability is

$$P_m(\delta_T - \delta^0) < \int_{\delta_T}^{\delta^u} P(u)du \tag{4.6}$$

4.3.3. Energy Functions for Multi Machine Power System

In this section energy functions for both synchronous reference frame and center of inertia reference frame are presented here and significance of each term in the energy function is presented.

4.3.3.1. Synchronous Reference Frame

The transient energy function V for the synchronous reference frame has the form [21]

$$V = \sum_{i=1}^{n-1}\sum_{j=i+1}^{n}\left[\frac{1}{2M_T}M_iM_j\left(\omega_i - \omega_j\right)^2 - \frac{1}{M_T}\left(P_iM_j - P_jM_i\right)\left(\delta_{ij} - \delta_{ij}^0\right)\right.$$

$$\left. -C_{ij}\left(cos\delta_{ij} - cos\delta_{ij}^0\right) + \int_{\delta_i^0+\delta_j^0-2\delta_0^s}^{\delta_i+\delta_j-2\delta_0} D_{ij}\cos\delta_{ij}d(\delta_i + \delta_j - 2\delta_0)\right] \tag{4.7}$$

Where

M_i = moment of inertia of machine *i*

ω_i = generator's *i* rotor speed

δ_i = generator's *i* rotor angle

δ_i^0 = generator's *i* SEP

$\delta_{ij} = \delta_i - \delta_j$

$\delta_0 = \frac{1}{M_T}\sum_{i=1}^{n} M_i \delta_i$

$P_i = P_{mi} - E_i^2 G_{ii}$

$C_{ij} = E_i E_j B_{ij}$

$D_{ij} = E_i E_j G_{ij}$

P_{mi} = mechanical power input

E_i = magnitude of voltage behind transient reactance

G_{ij} = real part of the *ij*th diagonal element of the network's *Y*-matrix

B_{ij} = imaginary component of the *ij*th element of the network's *Y*-matrix

Equation 4.7 can be used to calculate the total energy of the system after solving for δ_i's numerically. Equation 4.7 consists of four terms: the first term represents the total change in kinetic energy, the second term represents the total change in potential energy, the third term represents the total change in magnetic stored energy, and the fourth term represents the total change in dissipated energy

4.3.3.2. Center Of Inertia Reference Frame

Consider the system model represented by equations 3.28 and 3.29. The transient energy function V can be obtained by the *n(n-1)/2* relative acceleration equations, multiplying each of these by the corresponding relative velocity and integrating the sum of the resulting equations from a fixed lower limit of the SEP (denoted by δ^0) to a variable upper limit.

Equation 4.8 describes the energy V as a function of angular displacement δ and velocity ω [22].

$$V = \sum_{i=1}^{n-1} \sum_{j=i+1}^{n} [\frac{1}{2M_T} M_i M_j (\omega_i - \omega_j)^2 - \frac{1}{M_T}(P_i M_j - P_j M_i)(\delta_{ij} - \delta_{ij}^0) \\ -C_{ij}(cos\delta_{ij} - cos\delta_{ij}^0) + \int_{\delta_i^0+\delta_j^0-2\delta_0^s}^{\delta_i+\delta_j-2\delta_0} D_{ij} \cos\delta_{ij} d(\delta_i + \delta_j - 2\delta_0)] \quad (4.8)$$

Equation 4.8 can be rewritten

$$V = \frac{1}{2}\sum_{i=1}^{n} M_i \widetilde{\omega_i^2} - \sum_{i=1}^{n} P_i(\theta_i - \theta_i^0) - \sum_{i=1}^{n-1}\sum_{j=i+1}^{n}[C_{ij}(cos\theta_{ij} - cos\theta_{ij}^0) - \\ \int_{\theta_i^0+\theta_j^0}^{\theta_i+\theta_j} D_{ij} cos\theta_{ij} d(\theta_i - \theta_j)] \quad (4.9)$$

Where

M_i = moment of inertia of machine *i*

$\widetilde{\omega_i}$ = generator's *i* rotor speed relative to COI

θ_i = generator's *i* rotor angle relative to COI

θ_i^0 = generator's *i* SEP relative to COI

$\theta_{ij} = \theta_i - \theta_j$

P_i, C_{ij}, D_{ij} are defined in section 4.3.31

The terms of the TEF can be physically interpreted in the following way:

$$\text{KE} = \frac{1}{2}\sum_{i=1}^{n} M_i \widetilde{\omega_i^2} = \frac{1}{2}\sum_{i=1}^{n} M_i \omega_i^2 - \frac{1}{2}\sum_{i=1}^{n} M_T \omega_0^2$$

Total change in rotor *KE* relative to COI is equal to total change in rotor *KE* minus change in KE_{COI}.

$$\text{PE} = \sum_{i=1}^{n} P_i(\theta_i - \theta_i^0) = \sum_{i=1}^{n} P_i(\delta_i - \delta_i^0) - \sum_{i=1}^{n} P_i(\delta_0 - \delta_0^0)$$

Given that $\delta_0 \triangleq \frac{1}{M_T}\sum_{i=1}^{n} M_i\delta_i$, change in rotor PE relative to COI is equal to the change in rotor potential energy minus change in COI potential energy.

$C_{ij}\left(cos\theta_{ij} - cos\theta_{ij}^0\right)$ is the change in magnetic stored energy of the branch *ij*.

$\int_{\theta_i^0+\theta_j^0}^{\theta_i+\theta_j} D_{ij}cos\theta_{ij}d(\theta_i - \theta_j)$ is the change in dissipated energy of branch *ij*. This is path-dependent term and has to be computed by numerical integration if he system trajectory is known or can be computed. However, when critical energy is to be computed at a relevant UEP, the path from the SEP to UEP is not known. Hence, approximation is made by assuming a linear trajectory of the system between δ_i^s to δ_i^0. Thus we assume [23] [30]

$$\delta_i = \delta_i^s + p(\delta_i^0 - \delta_i^s)\,, \qquad p \in [0,1], (\mathrm{i} = 1,2,\ldots \mathrm{n}) \tag{4.10}$$

From equation 4.10, we get

$$d\delta_i = (\delta_i^0 - \delta_i^s)dp, i = 1,2,..,n \tag{4.11}$$

$$d(\delta_i + \delta_i) = \left(\delta_i^0 - \delta_i^s + \delta_j^0 - \delta_j^s\right)dp \tag{4.12}$$

$$d(\delta_i - \delta_i) = \left(\delta_i^0 - \delta_i^s + \delta_j^0 + \delta_j^s\right)dp \tag{4.13}$$

From equations 4.11, 4.12, 4.13

$$d(\delta_i + \delta_i) = \frac{\delta_i^0+\delta_j^0-\delta_i^s-\delta_j^s}{\delta_i^0-\delta_j^0-(\delta_i^s-\delta_j^s)}\,d(\delta_i - \delta_i) \tag{4.14}$$

By eliminating *dp*. And substituting equation 4.14 in the change in dissipated energy term of TEF V, we get

$$\sum_{i=1}^{n-1}\sum_{j=i+1}^{n}\left[\int_{\theta_i^0+\theta_j^0}^{\theta_i+\theta_j} D_{ij}cos\theta_{ij}d(\theta_i - \theta_j)\right] = -\sum_{i=1}^{n-1}\sum_{j=i+1}^{n} D_{ij}\,\frac{\delta_i^0+\delta_j^0-\delta_i^s-\delta_j^s}{\delta_i^0-\delta_j^0-\left(\delta_i^s-\delta_j^s\right)}\left[sin\delta_{ij}^0 - sin\delta_{ij}^s\right] \tag{4.15}$$

From the above discussion, it is clear that the change in energy associated with motion of the system COI is subtracted from the total system energy in order to obtain the TEF.

4.3.3.3. Transient Stability Assessment Methods

1) Potential Energy Boundary Surface [23]

The concept of PEBS was first mooted by Kakimoto et al. (1978) as a set of curves passing through UEPs and orthogonal to the equipotential curves. The significance of PEBS is in the context of suggestions made by Kakimoto et al. (1978) and Athay et al. (1979) that it is better to use the CUEP instead of the closest UEP to estimate the stability domain [31] [32]. The CUEP lies on the PEBS through which the unstable trajectory leaves the stability region. The point of intersection of the unstable trajectory with the PEBS is called the "exit point." Mathematically, PEBS is defined by the points that satisfy the relation that the directional derivative of the PE function along the rays emanating from SEP is zero. Thus, the following equation characterizes PEBS (Athay et al. 1979) [28] [29]:

$$\sum_{i=1}^{n-1} f_i(\delta)(\delta_i - \delta_i^s) = 0 \qquad (4.16)$$

The advantage of PEBS as originally defined by Kakimoto et al. (1978) is that a simple procedure for the computation of stability boundary can be given. The computation of the CCT is given below:

Step 1: Integrate the fault-on trajectory until W_{PE}reaches a local maximum. This value is an estimate of the true W_{cr}.

Step 2: From the fault-on trajectory, determine the instant when $W = W_{cr}$. This is the CCT (*tcr*). Figure 2.9 shows this graphically.

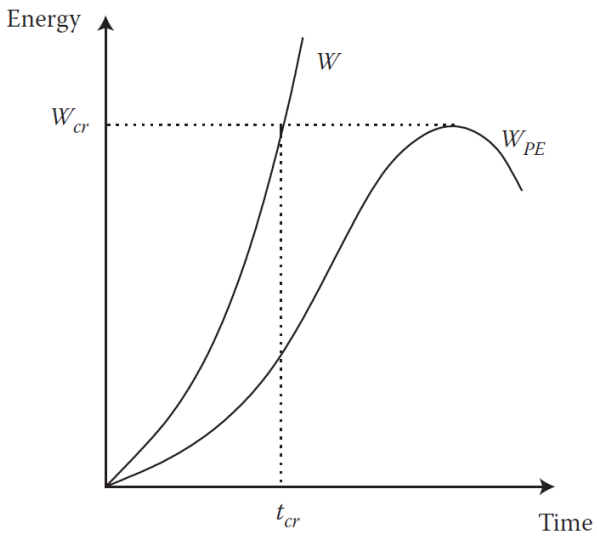

FIGURE 4.2: Determination of critical clearing time using PEBS. Redrawn from [23]

2) Controlling Unstable Equilibrium Point method(CUEP) [23]

In this method, the critical energy is determined as

$$W_{cr} = W(x_u^*) = W_2(d_u^*) \tag{4.17}$$

Where x_u^* is the type 1 UEP lying on the stability boundary and whose stable manifold is intersected by the fault-on trajectory. As the rotor velocity deviation, ω, is zero at any equilibrium point, the critical energy is the same as the PE W_2 evaluated at the value d_u^* corresponding to the CUEP. The determination of CUEP can be complex. There are several approaches to the determination of CUEP. Two prominent approaches that have been applied for large systems are

1. Mode of disturbance (MOD) (Fouad and Vittal 1992)

2. BCU method (Chiang et al. 1994)

3) Boundary of Stability Region-Based Controlling Unstable Equilibrium Point [23].

The BCU method was proposed by Chiang et al. (1994). This method is based on the relationship between the stability boundary of the (postfault) classical power system model and the stability boundary of the following (postfault) reduced system model defined as

$$\dot{\delta} = f(\delta) \tag{4.18}$$

The state variables of this reduced system are rotor angles only with dimension of *n* while the dimensions of the original system is 2*n*. It is easy to that if $\hat{\delta}$ is an EP of the system defined by equation 4.18, then ($\hat{\delta}$,0) is an EP of the original system. Under the condition of small transfer conductances, it can be shown that

1. ($\widehat{\delta^s}$) is an SEP of the reduced system if and only if ($\widehat{\delta^s}, 0$) is an SEP of the original system.

2. ($\widehat{\delta^0}$) is a type-k EP of the reduced system if and only if ($\widehat{\delta^0}, 0$) is a type-k EP of the original system.

3. If the one-parameter transversality condition is satisfied, then ($\widehat{\delta}$) is on the stability boundary $\partial A(\widehat{\delta^s})$ of the reduced system if and only if ($\widehat{\delta^s}, 0$) is on the stability boundary $\partial A(\widehat{\delta^s}, 0)$ of the original system.

The above results establish a relationship between the stability boundary $\partial A(\widehat{\delta^s})$ and the stability boundary ($\widehat{\delta^s}, 0$) , and suggest a method of finding the CUEP of the original system via the location of CUEP of the reduced system. In this thesis PEBS method is used to determine CCT.

4.3.4. Test System and Simulation Results

WSCC 9 bus test system presented in figure 3.7.1 is used for simulations and equations in section 4.3.3.2 are used for calculating total kinetic energy and total potential energy of the system during a disturbance. COI reference frame is used for generators and loads are modeled as constant impedance load. Moreover, the system stability was predicted from KE, PE and total energy. Critical clearing time of the system is predicted using PEBS method.

Case 1: Same disturbance is created as in case 4 in section 3.7.3 on WSCC system. And total kinetic energy and potential energy are computed.

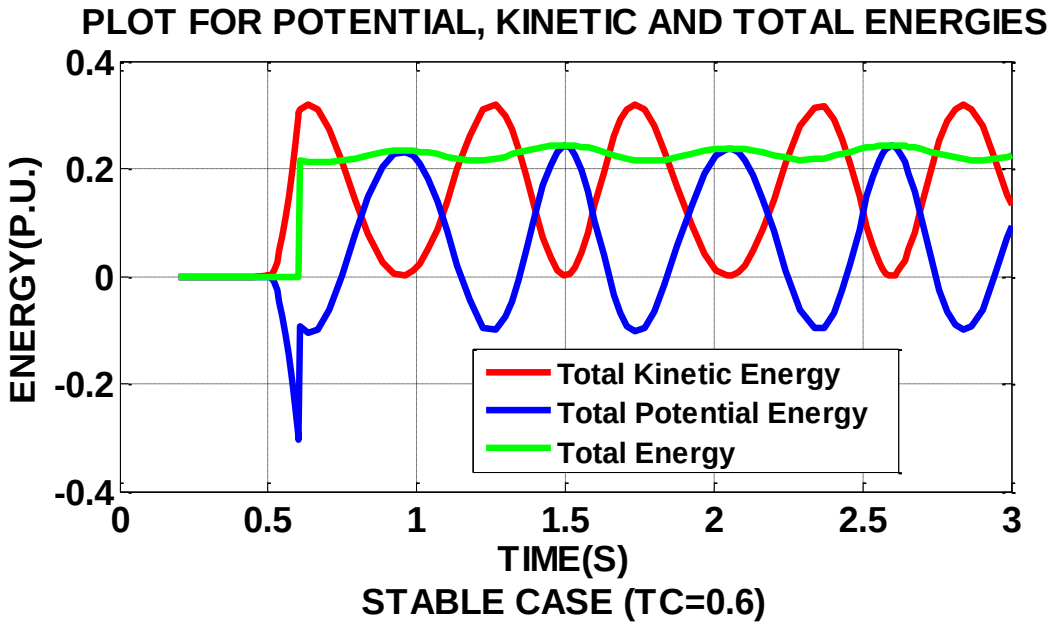

FIGURE 4.3: Plot for PE, KE, TE (stable case, tc=0.6)

Case 2: Same disturbance is created as in case 5 in section 3.7.3 on WSCC system. And total kinetic energy and potential energy are computed.

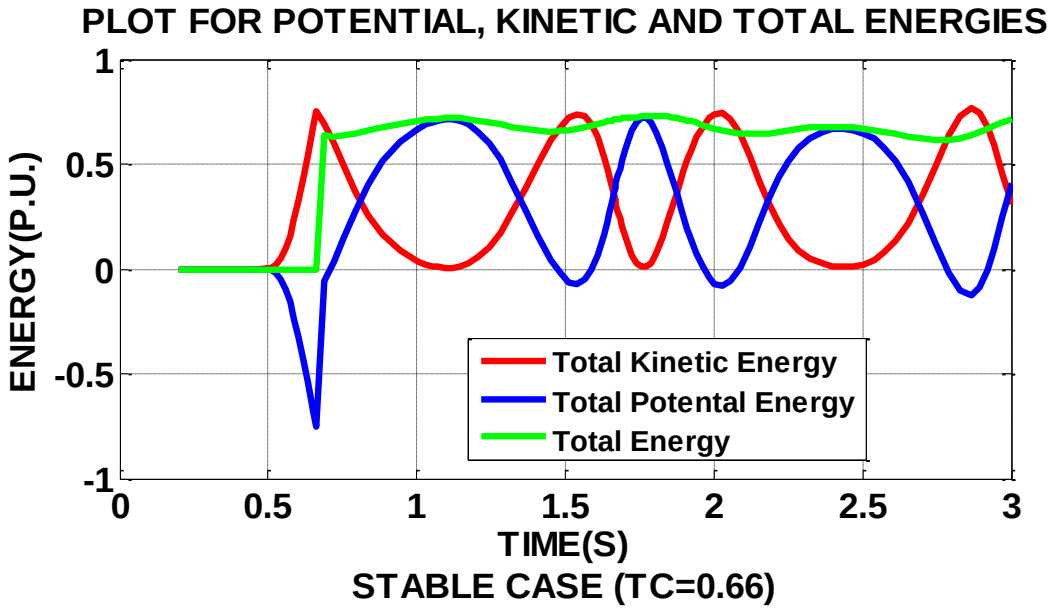

FIGURE 4.4: Plot for PE, KE, TE (stable case, tc=0.66)

Case 3: Same disturbance is created as in case 6 in section 3.7.3 on WSCC system. And total kinetic energy and potential energy are computed.

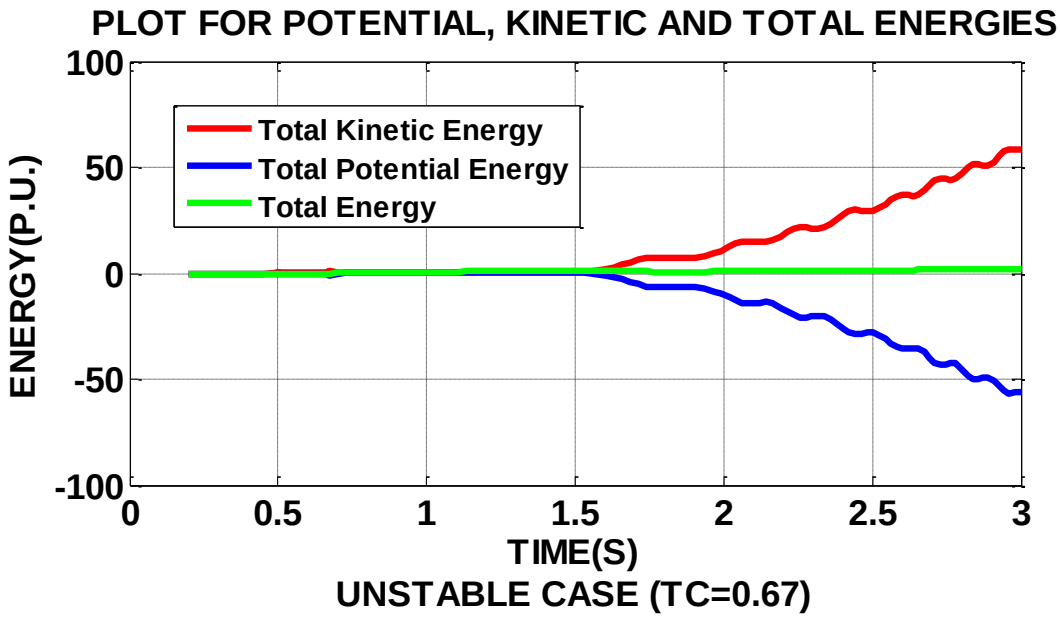

FIGURE 4.5: Plot for PE, KE, TE (unstable case, tc=0.67)

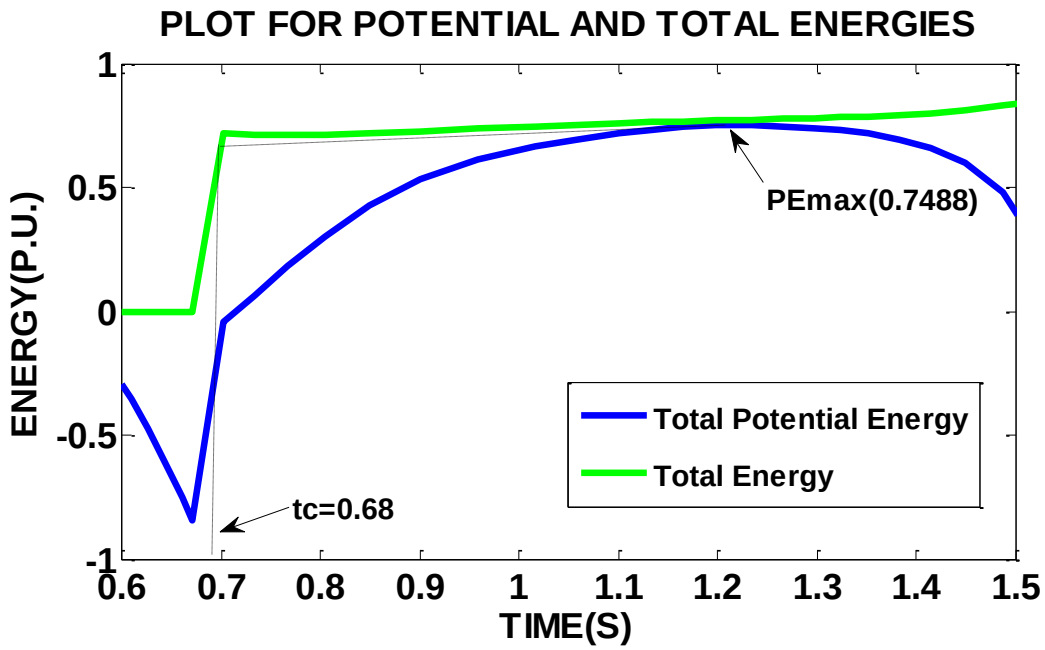

FIGURE 4.6: Critical clearing time determination from PEBS method

Case 4: Faults are created at different locations on WSCC 9 bus test system and critical clearing time is computed and compared with numerical methods. Table 4.1 below shows comparison between results obtained from direct and numerical methods.

TABLE 4.1: Comparison of critical clearing time obtained from numerical and direct methods.

Case	Fault At Bus	Line Tripped	Critical Clearing Time(sec)	
			Numerical Method	Direct Method
1	7	No line tripped	0.74	0.75
2	7	5-7	0.67	0.68
3	9	No line tripped	0.25	0.25
4	9	6-9	0.21	0.23
5	8	No line tripped	0.33	0.31
6	8	8-7	0.3	0.3

4.3.5. Simulation Results Analysis

Transient stability analysis is done on WSCC 9-bus test system by energy functions formulated in section 4.3.3 and simulation results are compared with numerical methods. Main observations are

- From figures 4.3 to 4.5 we can see that for a stable case both potential and kinetic energies are bounded. Moreover, for a stable case the system converts the increased kinetic energy, due to a disturbance into potential energy and maintains the system stability. But when the disturbance is large then the system fails to convert increased kinetic energy into potential energy and all the energy in the system is gradually converted into kinetic energy and system loses its stability.
- From PEBS method we can determine the critical clearing time by determining the maximum PE of the system on PE plot and its intersection with the total energy.
- Critical clearing time predicted by conventional numerical methods are similar to critical clearing time obtained from direct methods.
- For larger systems use of direct methods would be more efficient than numerical methods because direct methods reduce computational time and asses transient stability of the system faster.

4.4. Summary

In this chapter, concepts of direct methods and its applications for transient stability studies are explained in detail. Also, transient energy functions are discussed. Moreover, total energy, potential energy and kinetic energy are plotted and stability of the system is predicted. The clearing time determined from direct methods are compared with clearing time obtained from time domain simulations.

In Chapter 5, concepts of structure preserving networks are discussed and equations for structure preserving networks are derived. Also, effect of load models on the stability of the system are discussed and transient energy functions for structure preserving network with frequency dependent loads are presented.

CHAPTER 5 : STRUCTURE PRESERVING ENERGY FUNCTIONS BASED DIRECT METHOD FOR TRANSIENT STABILITY ANALYSIS

This chapter presents structure preserving power system models and energy functions. Section 5.1 and Section 5.2 presents the overview and theory of structure preserving models. Effect of load models are presented in Section 5.3. Structure preserving energy functions and simulation results are presented in Section 5.4 Section 5.5. Summary of the chapter is presented in Section 5.7

5.1. Overview

Most of the literature on Lyapunov-like energy functions assume linear voltage-dependent load models that enable the reduction of power system network, retaining only the generator internal nodes. The transfer conductances (TCs) in the reduced admittance matrix of the network are neglected to construct the energy function. It is to be noted that although the transmission network can be reasonably modeled as lossless, the TCs are mainly introduced due to the load impedances with substantial resistive components. A major disadvantage of using reduced bus admittance matrix is that the original network topology is lost. This has two adverse effects: (1) the network controllers such as HVDC converter and FACTS controllers cannot be satisfactorily modeled and (2) the application of electrical circuit or network theory concepts is not feasible [23].

5.2. Structure Preserving Power System Models for Transient Stability Studies [24]

While many of the assumptions made to arrive at the usual classical model for transient stability analysis are reasonable, that of ignoring transfer conductances is usually quite

crude. This emanates from modeling the loads as impedances (with a substantial resistive component). These are then absorbed into the bus admittance matrix for a reduced network based on generator buses. Thus, although the original transmission network is very reasonably modeled as lossless, the reduced network certainly cannot be in general. Consequently, a path-independent potential function is not readily available for constructing Lyapunov functions. Attempts to develop general Lyapunov functions have met very limited success, especially when it is considered that ultimately these functions should replace those based on assuming the conductances are zero. Pai and Murthy have a Lyapunov function for the two machine case, but a generalization has inherent difficulties. Jocic et. al. report an approach based on large-scale systems theory, but a clear improvement in practice is not achieved. The inclusion of transfer conductances is sometimes handled by some approximation, either in the system description or in evaluating the 'Lyapunov function' (or transient energy function) [33]. A further disadvantage of forming a reduced network (by suppressing load buses) is that the original network topology is lost. This can mask the role of structural aspects in stability assessment. Bergen and Hill (1981) proposed an SPM for stability analysis by retaining the identity of the load nodes, which also preserved the structure of the transmission network. The active loads were modeled as frequency dependent, but independent of the bus voltages. They assumed that the relationship with frequency is linear.

The formulation assumed that [23]

1. The transmission network is lossless

2. The network has *n* buses with constant voltage magnitudes, which are all assumed to be equal to 1

3. The load model is given by

$P_{Di} = P_{Di}^{0} + D_i\dot{\delta_i} \quad i = m+1, \ldots, n$

Where

P_{Di}^{0} = mean value of the active power

5.2.1. Structure Preserving Multi Machine Power System Model

In this section, a model of a multi machine power system is developed. Loads are not assumed as constant impedance loads, which are absorbed into the transmission network. A four bus power system is with two generators and three loads is considered. The system shown in Figure 5.1 In general, suppose there are m generators and $n_0$buses in the physical system, with n_0-m buses having loads and no generation. It is convenient to introduce fictitious buses representing the internal generation voltages [34] [35]. These are connected to the generator buses via reactances accounting for transient reactances and connecting lines. Thus in the augmented network there is a total of n=m+n_0 buses. We number the fictitious generator buses l,..., m, the corresponding physical buses m+l,...,2m and the remaining load buses 2m+l, ...,n. Suppose that within the transmission network there are l_0 lines [36]. Then l_0 must satisfy $l_0 \leq \frac{1}{2}n_0(n_0 - 1)$ and the total number of lines in the augmented network is $l = m + l_0$. We number the transmission network lines 1,…, l_0 and the generator bus lines $l_0 + 1$,…..,l connected to buses 1,….m respectively. The nth bus will be used as a reference. For the four bus example, Figure 5.2 shows the augmented network. At this stage, it is useful to recognize that the network is analogous to a nonlinear resistive network with real power corresponding to current and the angle difference across a line corresponding to branch voltage. Assuming a lossless transmission network and $\sum_{i=1}^{n} P_i = 0$,where P_i is the injected power at bus i, Kirchhoff's laws hold in the obvious

sense. For the four bus example, the analogous circuit is shown in figure 5.3 [37] [38]. The nonlinear resistance characteristic for each branch is given by the familiar power-angle relationship for a line. We assume that the graph for the network is connected and planar and the branches are oriented according to associated reference directions [24].

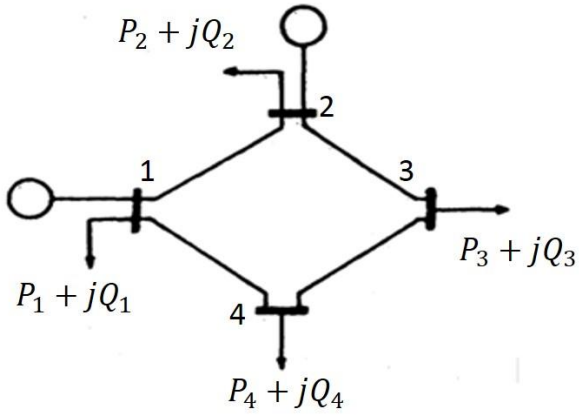

FIGURE 5.1: Four bus power network

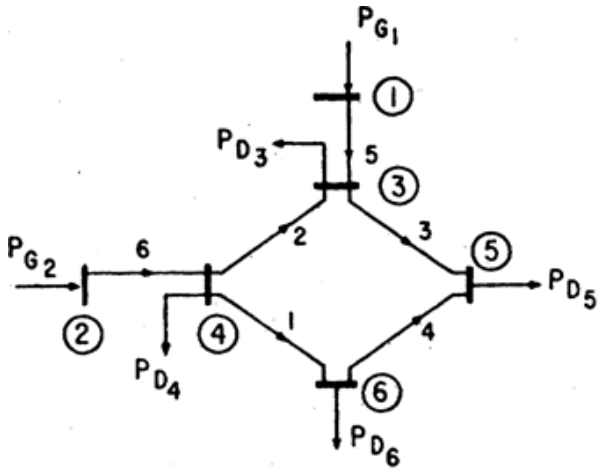

FIGURE 5.2: Augmented network with generator bus lines

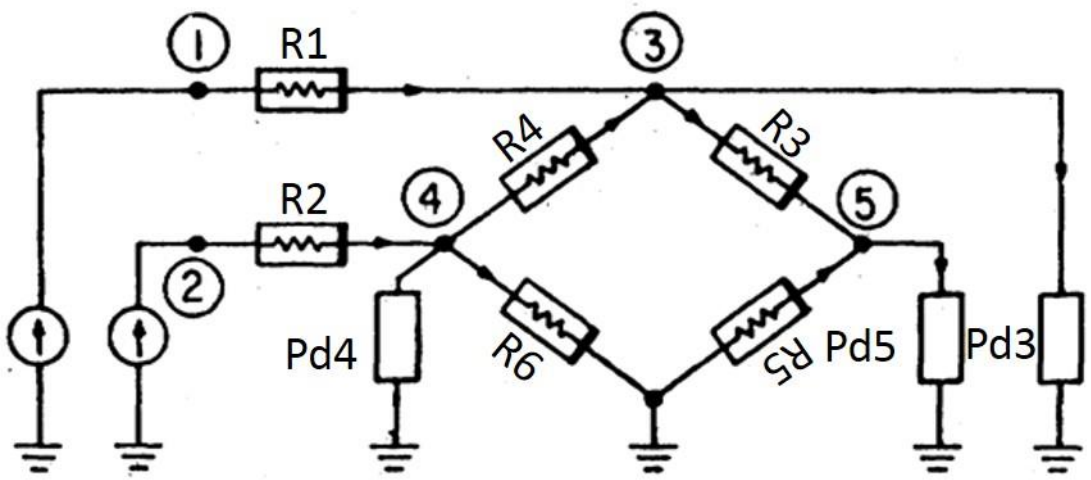

FIGURE 5.3: Analogous nonlinear resistive circuit

Now the key assumptions of the dynamic loads is introduced. Let P_{Di} be the real power drawn by the load at bus i. in general P_{Di} is a nonlinear function of voltage and frequency. For constant voltages and small frequency variations around the operating point P_{Di}^0, it is reasonable to assume

$$P_{Di} = P_{Di}^0 + D_i\delta_\iota \quad \iota = \dot{m} + 1, \dots, n \tag{5.1}$$

Where D_i>0. Note that as $D_i \to 0^+$ we obtain a constant load model. This load frequency dependence is usually assumed in modeling the power-frequency control system, but has not been used in modeling for transient stability. Using equation 5.1 and swing equations in chapter 2.1 we can write

$$M_i\ddot{\delta}_\iota + D_i\dot{\delta}_\iota + \sum_{\substack{j=1 \\ j\neq i}}^{n} b_{ij}\sin(\delta_i - \delta_j) = P_{mi}^0 - P_{Di}^0 \triangleq P_i^0 \;\; i = 1, \dots n \tag{5.2}$$

Where

$M_i > 0$ i=1,…m (generator inertia constant)

$M_i = 0$ i=m+1,..,n

$D_i > 0$ i=1,….,m (steam and mechanical damping of generator)

$D_i > 0$ i=1,….,m (frequency coefficient of load)

$P_{Di}^0 = 0$ i=1,….,m

$P_{mi}^0 = 0$ i=1,….,m

Equation 5.2 looks similar to the usual classical swing equation model used in previous studies of transient stability via Lyapunov methods. However, there are important differences. Along with the mechanical input powers P_{mi}^0, the loads P_{Di}^0 are shown explicitly. Consequently, the network topology is preserved just as in the case of the load flow model.

5.3. Effect of Load Models

The characteristics of the loads influence the system stability and dynamics in many different ways. The voltage characteristics of the loads have a direct influence on the accelerating power for generators nearby and are thus very important for the behavior during the first oscillation after a fault. The frequency dependency of the loads also influences the system damping. The same is true for their voltage dependency since it influences the voltage control. It is for several reasons difficult to derive good load models. (Of course, deriving models for single load objects is formally not very difficult. Loads here are, however, lumped loads as they are perceived from a bus in the high voltage grid.) First, it is difficult to estimate the composition of the loads, since it varies during the day as well as during the year. Further, this composition varies from bus to bus. Thus, sometimes different load models have to be used at different buses, depending on the composition of the loads, for example industrial loads, domestic loads, and rural loads. For studies of angular stability, loads are usually modelled with static models. Sometimes, large induction motors have to be represented individually by special models to obtain the correct

dynamic behavior. Dynamic load models for lumped loads have begun to be used during the last few years, especially for studying voltage stability, but those are expected to be used in the future more widely and even for other types of studies [25][39].

5.4. Structure Preserving Transient Energy Function with Frequency Dependent Loads

To accurately include the effects of the loads in the system, the so-called structure preserved, center of inertia model of the power system is used. The generator equations 5.2.1 can be rewritten as equation 5.4 to obtain generator equations with respect to COI reference frame [26] [40].

$$\dot{\theta}_\iota = \widetilde{\omega_\iota} \tag{5.3}$$

$$M_i\dot{\widetilde{\omega_\iota}} = P_{mi} - \sum_{j=1}^{n} B_{ij}V_iV_j \sin\left(\theta_i - \theta_j\right) - \frac{M_i}{M_T}P_{COI} \tag{5.4}$$

i=1,….m for equation 5.3 and 5.4

$$0 = P_{di}^0 + D_i\dot{\theta}_\iota + \sum_{j=1}^{n} B_{ij}V_iV_j \sin\left(\theta_i - \theta_j\right) \tag{5.5}$$

$$0 = Q_{di} + \sum_{j=1}^{n} B_{ij}V_iV_j \cos\left(\theta_i - \theta_j\right) \tag{5.6}$$

i=m+1,…n for equation 5.5 and 5.6

Where

$$\theta_i = \delta_i - \delta_0 \tag{5.7}$$

$$\widetilde{\omega_\iota} = \omega_i - \omega_0 \tag{5.8}$$

$$\delta_0 = \frac{1}{M_T}\sum_{i=1}^{m} M_i\,\delta_i \tag{5.9}$$

$$\omega_0 = \frac{1}{M_T}\sum_{i=1}^{m} M_i\,\omega_i \tag{5.10}$$

$$M_T = \sum_{i=1}^{m} M_i \tag{5.11}$$

$$P_{COI} = \sum_{i=1}^{m}\left(P_{mi} - \sum_{j=1}^{n} B_{ij}V_iV_j \sin\left(\theta_i - \theta_j\right)\right) \tag{5.12}$$

δ_i = generator rotor angle

θ_i = COI bus angle

ω_i = generator angular frequency

$\widetilde{\omega_\iota}$ = COI angular frequency

M_i = inertia constant

P_{mi} = mechanical output

V_i = bus voltage

B_{ij} = (i,j) th entry of the reduced lossless admittance matrix

D_i = positive sensitivity coefficient representing the load frequency dependence

m = number of generators in the system

n = number of total buses in the system

P_{di} and $Q_{di}$are the load demands at each bus i in the system

The corresponding energy function is [26]

$$V\left(\widetilde{\omega_{g\iota}},\theta,V\right)=\underbrace{\frac{1}{2}\sum_{i=1}^{m}M_i\,\widetilde{\omega_{g\iota}}}_{KE}-\underbrace{\sum_{i=1}^{m}P_{mi}\,(\theta_i-\theta_i^s)}_{PE\,1}+\underbrace{\sum_{i=1}^{n+m}P_{di}\,(\theta_i-\theta_i^s)}_{PE\,2}-$$

$$\underbrace{\frac{1}{2}\sum_{i=1}^{n+m}B_{ii}\,(V_i^2-(V_i^s)^2)}_{PE\,3}+\underbrace{\sum_{i=1}^{n+m}\frac{Q_{di}^s}{a(V_i^s)^a}\,(V_i^a-(V_i^s)^a)}_{PE\,4}-$$

$$\underbrace{\sum_{i=1}^{n+m-1}\sum_{j=i+1}^{n+m}B_{ij}\left(V_iV_j\cos\left(\theta_i-\theta_j\right)-V_i^sV_j^s\cos\left(\theta_i{}^s-\theta_j{}^s\right)\right)}_{PE\,5} \qquad (5.14)$$

Where “a” is usually 2 and the superscript “s” indicates the stable equilibrium point.

Total PE= PE1+PE2+PE3+PE4+PE5.

Total Energy = KE+PE

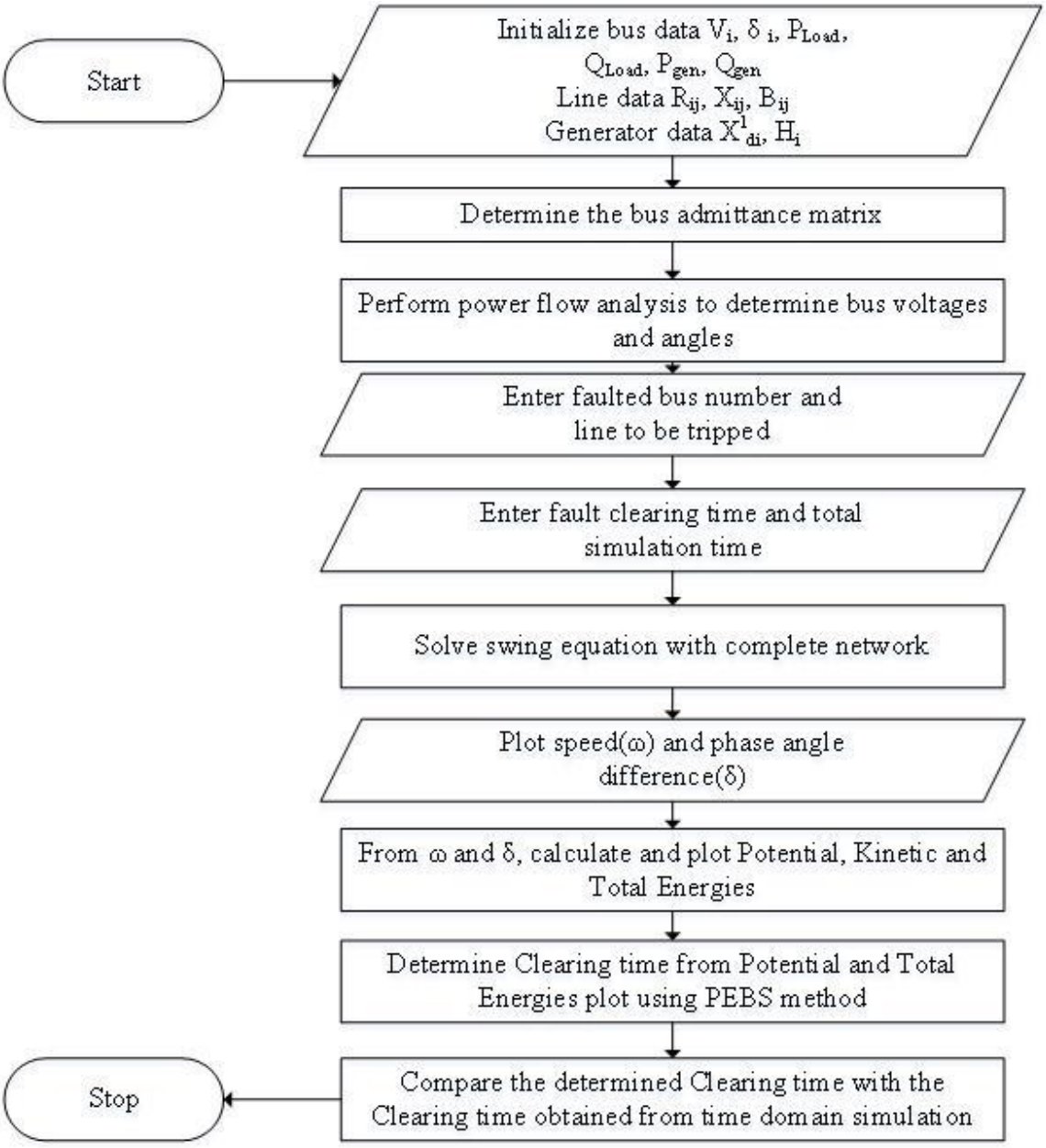

FIGURE 5.4: Flow chart for determining critical clearing time of structure preserved network using PEBS method.

5.5. Test System and Simulation Results

WSCC 9 bus test system, New England 39 bus test system and NETS-NYPS 68 bus test system are used for simulations. Structure preserving models and frequency dependent loads are used instead of conventional reduced networks with constant impedance loads.

Case 1: Analysis on small power grid

Same disturbance is created as in case 4 in section 3.7.3 on WSCC system. Comparison of rotor angles and speed with respect to center of inertia reference frame, for reduced and structure preserved network was done.

SP = Structure Preserved network

R = Reduced network

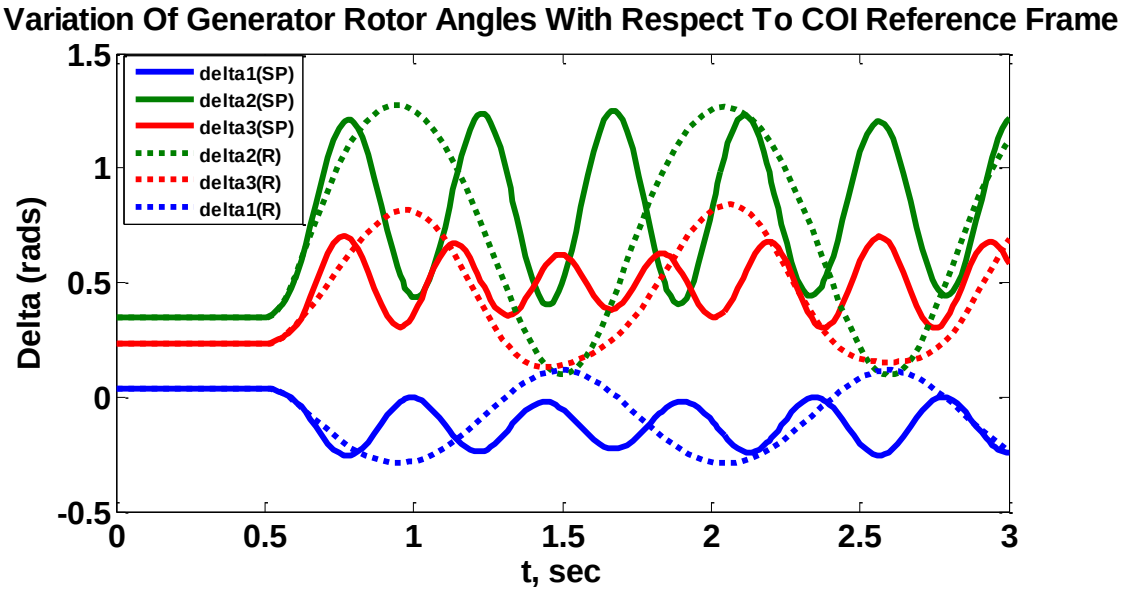

FIGURE 5.5: Comparison of rotor angle variation with reduced and structure preserved network

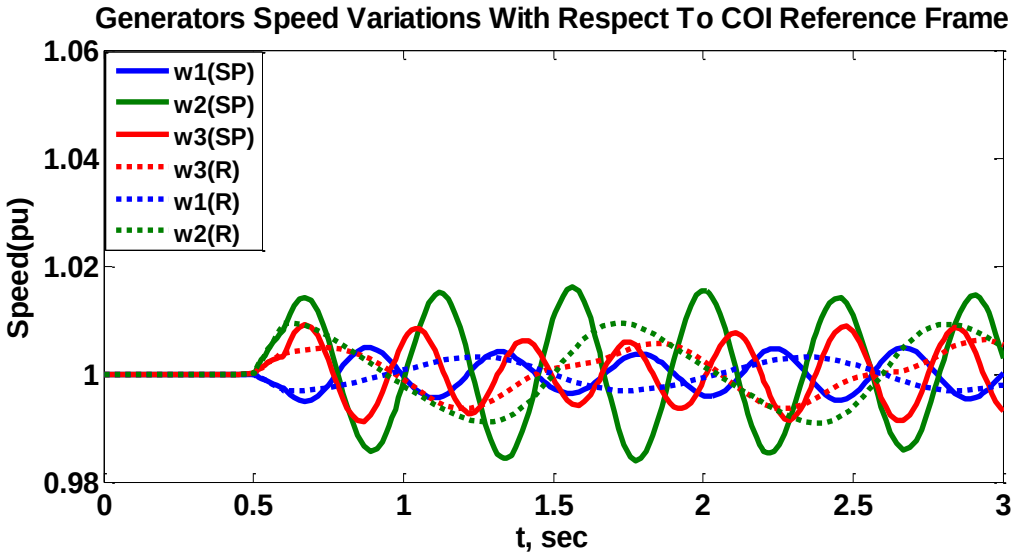

FIGURE 5.6: Comparison of generator speed variation with reduced and structure preserved network

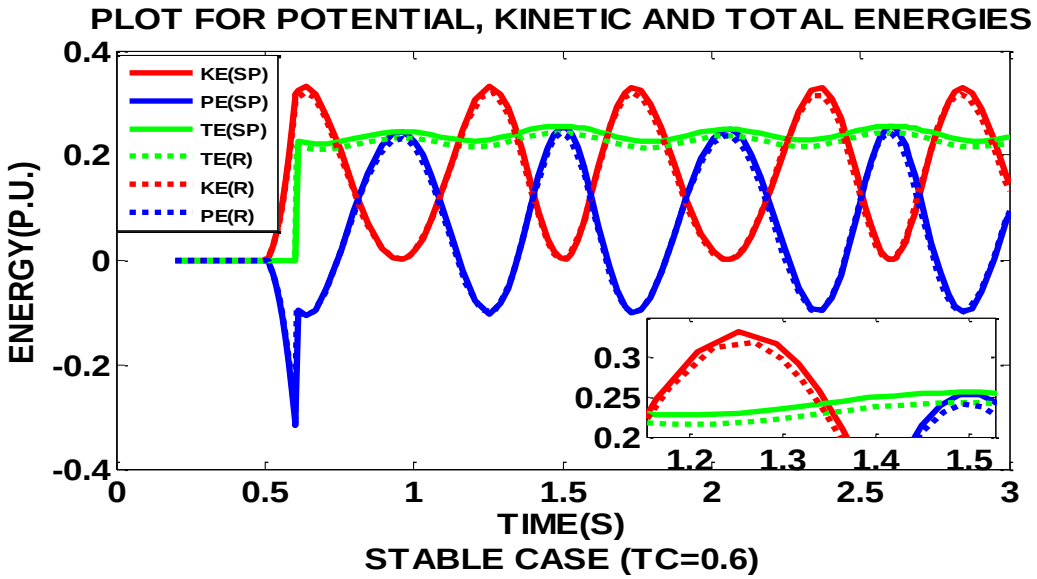

FIGURE 5.7: Comparison of PE, KE and TE with reduced and structure preserved network

Case 2: Analysis on large scale power grid –IEEE 39 BUS TEST SYSTEM

New England 39 bus test system is used refer Appendix A for 39 bus test system data. The network structure was preserved and frequency dependent loads are used. A three phase fault is applied close to bus 5 at 0.1 sec and fault is cleared at 0.2 by removing line 5-8. Refer to appendix B for generator rotor angles and speed variation with respect to COI reference frame.

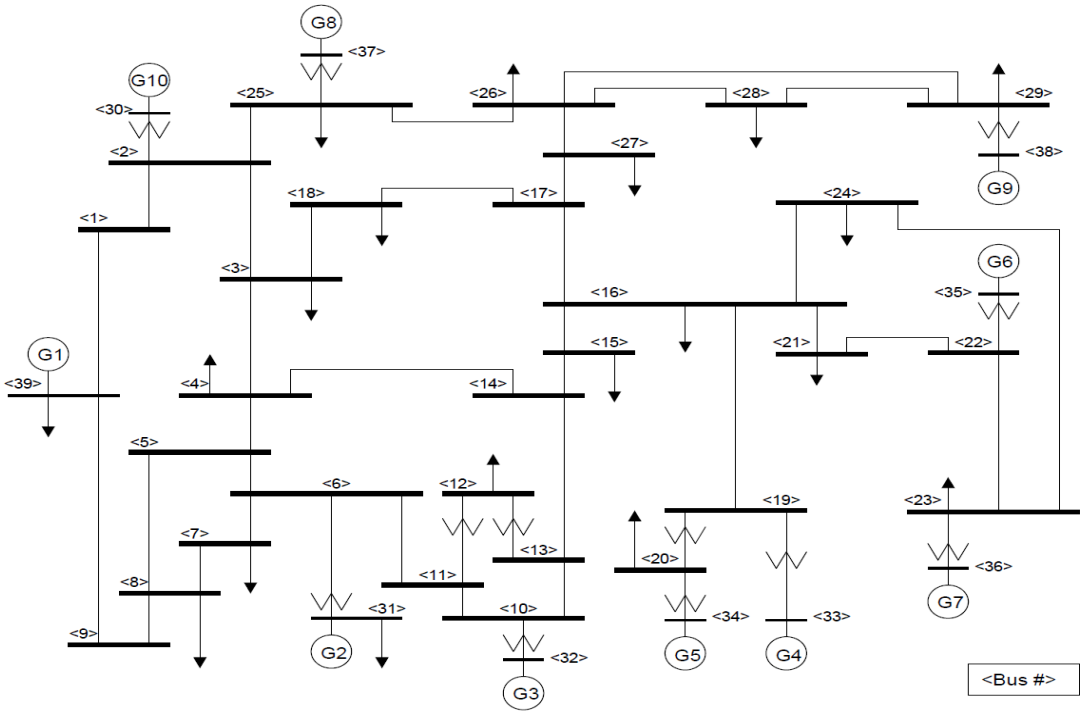

FIGURE 5.8: Single line diagram of 39 bus test system

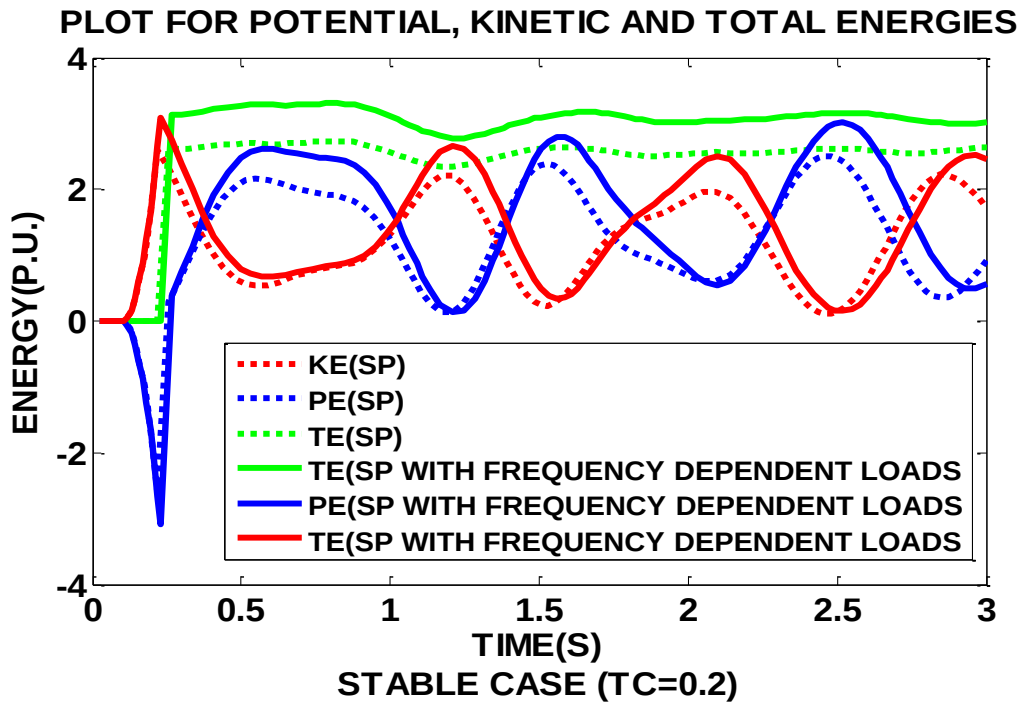

FIGURE 5.9: Comparison of PE, KE and TE of structure preserved network with and without frequency dependent loads

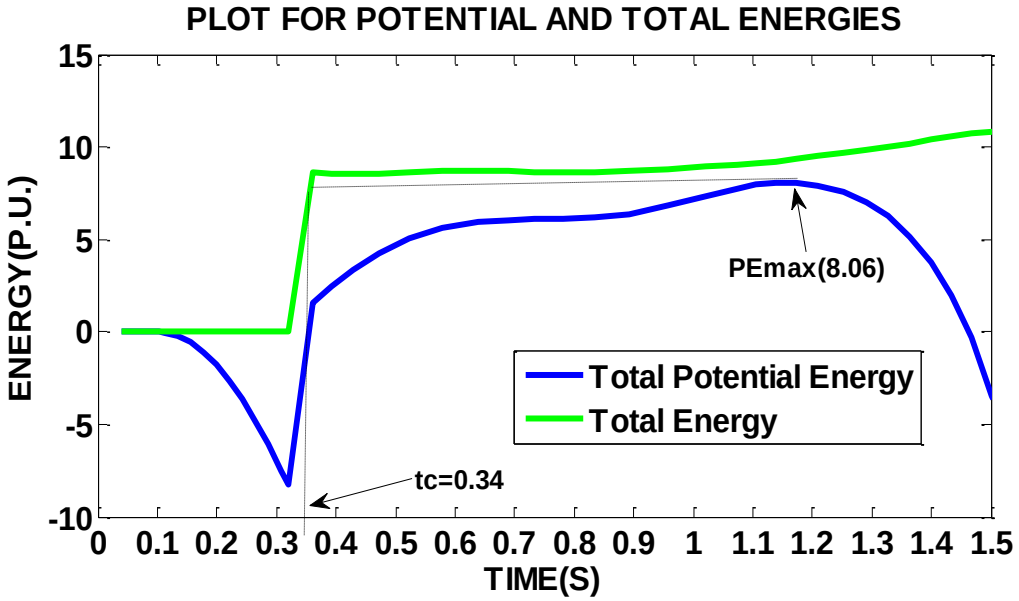

FIGURE 5.10: Critical clearing angle determination using PEBS method for system with frequency dependent loads

Case3: Analysis on large scale power grid-IEEE 69 BUS TEST SYSTEM

NETS-NYPS 68 bus test system is used refer Appendix A for 68 bus test system data. Both reduced model and structure preserving model with frequency dependent loads are used. A three phase fault is applied close to bus 32 at 0.5 sec and fault is cleared at 0.6 by removing line 32-30.

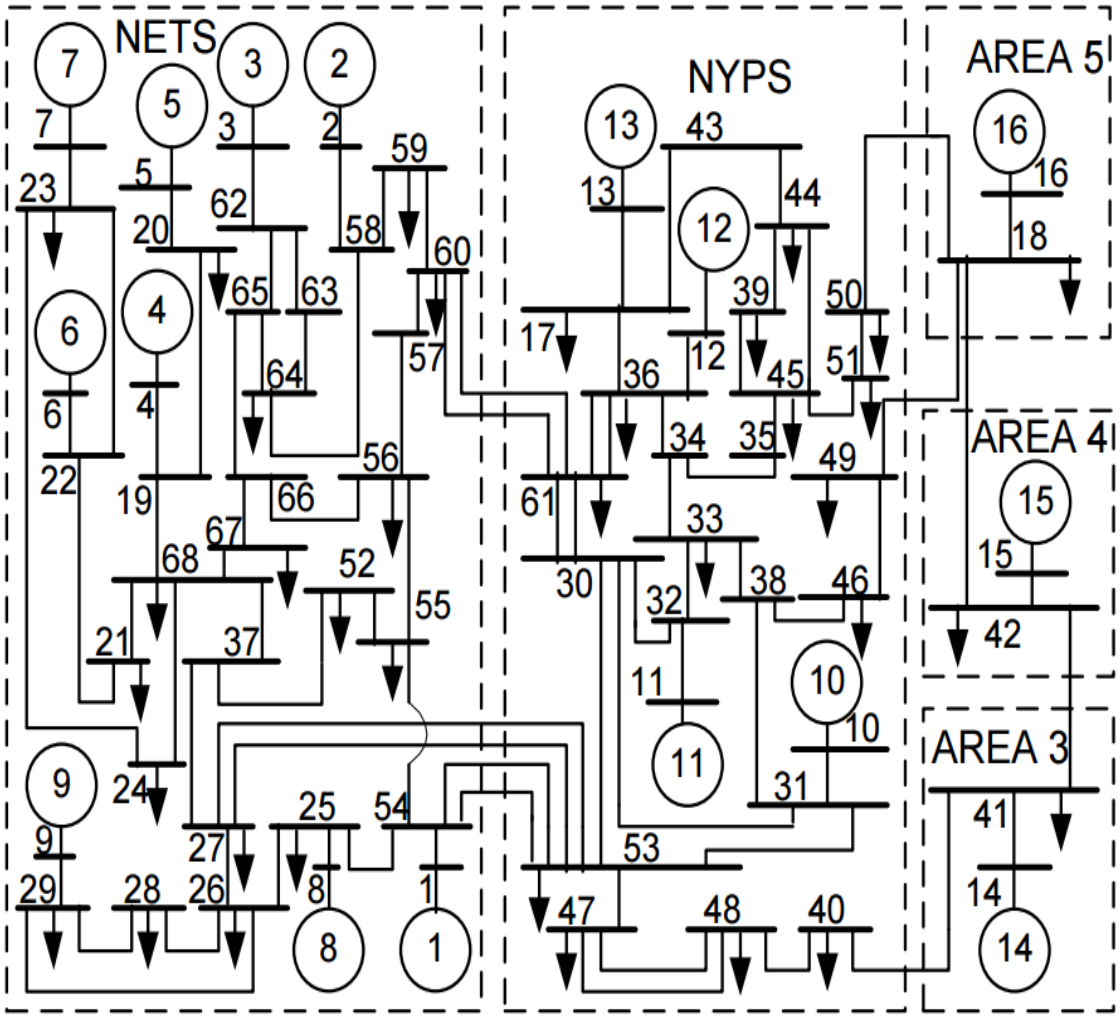

FIGURE 5.11: Single line diagram of NETS-NYPS 68 bus test system

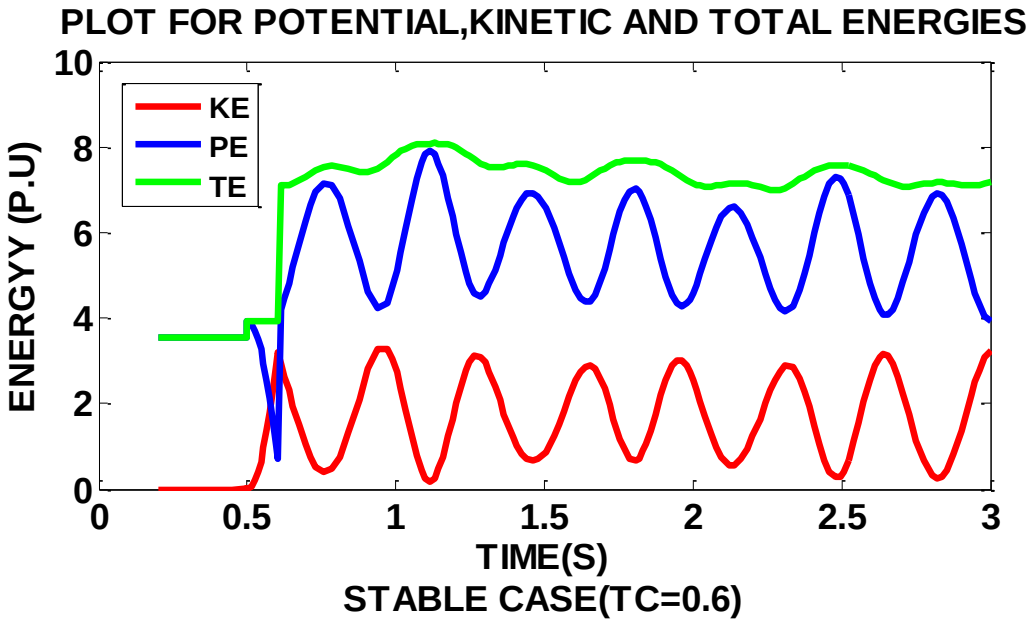

FIGURE 5.12: Plot for Potential, Kinetic and Total energies of a reduced network, stable case.

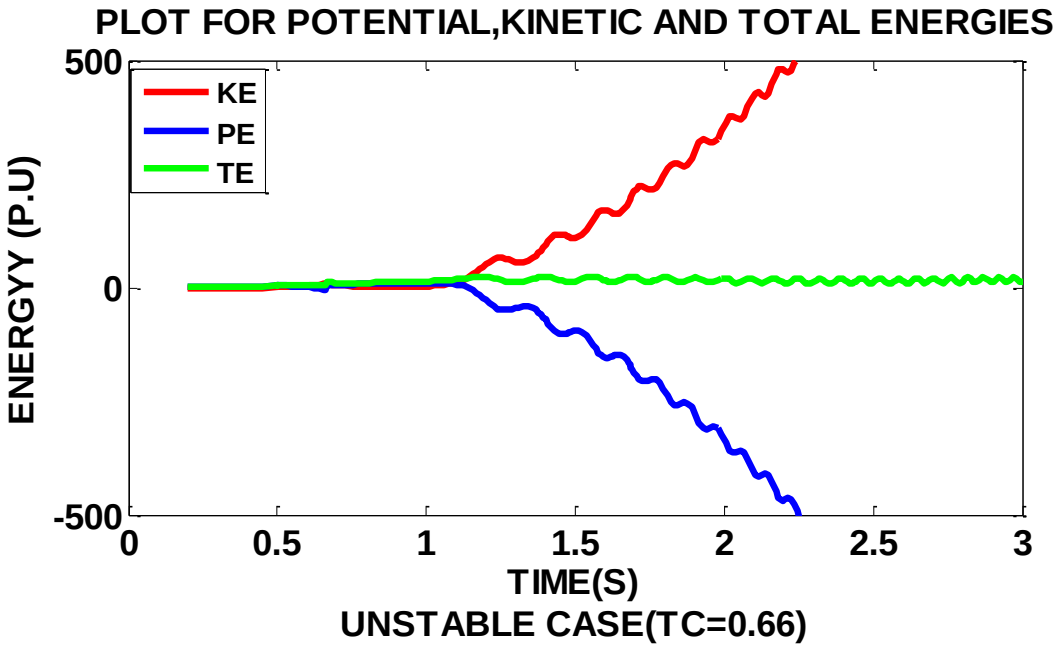

FIGURE 5.13: Plot for Potential, Kinetic and Total energies of a reduced network, unstable case.

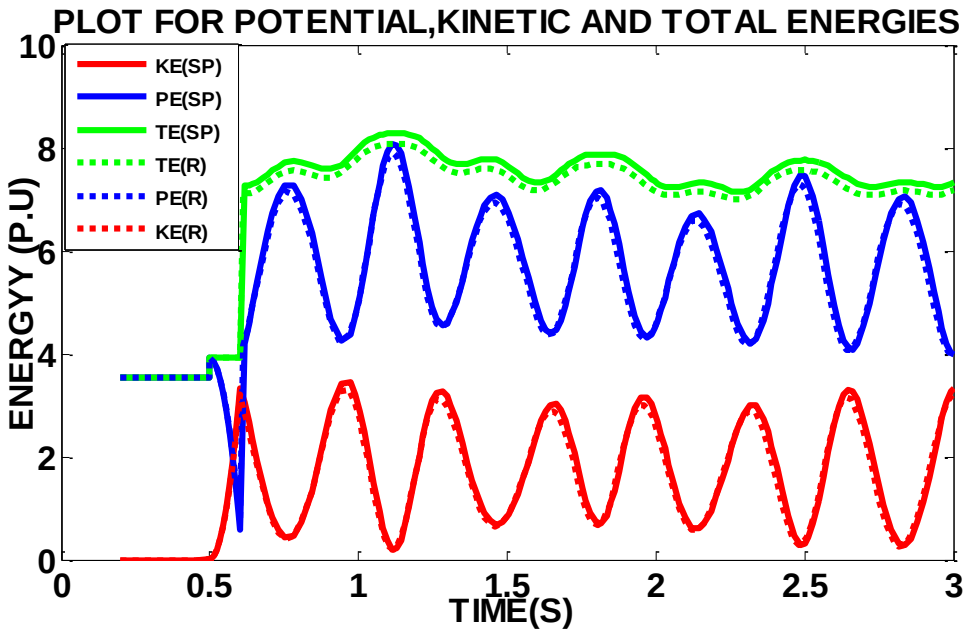

FIGURE 5.14: Comparison of PE, KE and TE with reduced and structure preserved network

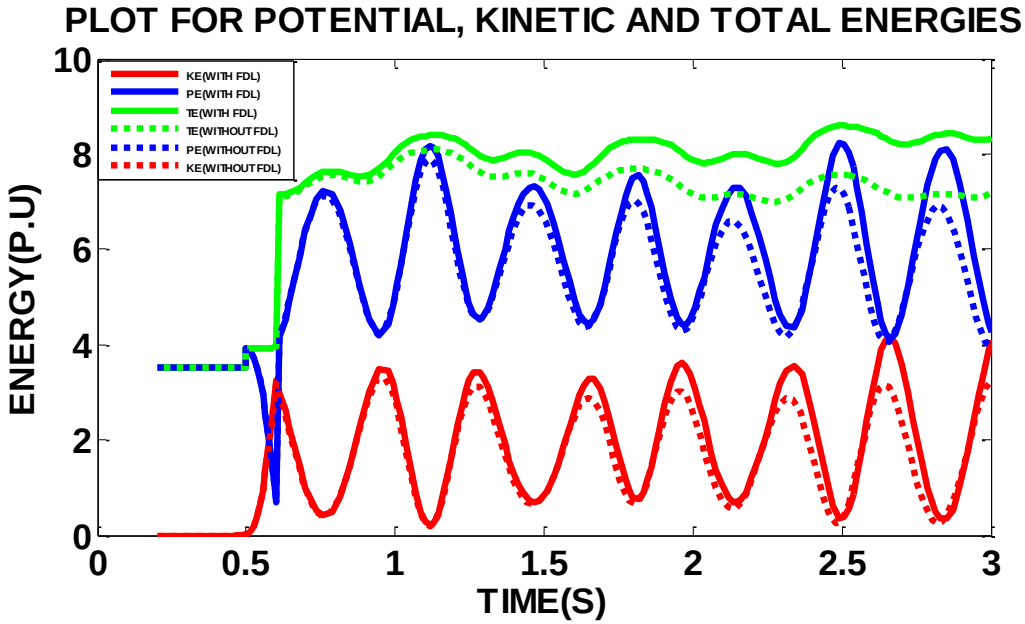

FIGURE 5.15: Comparison of PE, KE and TE of structure preserved network with and without frequency dependent loads

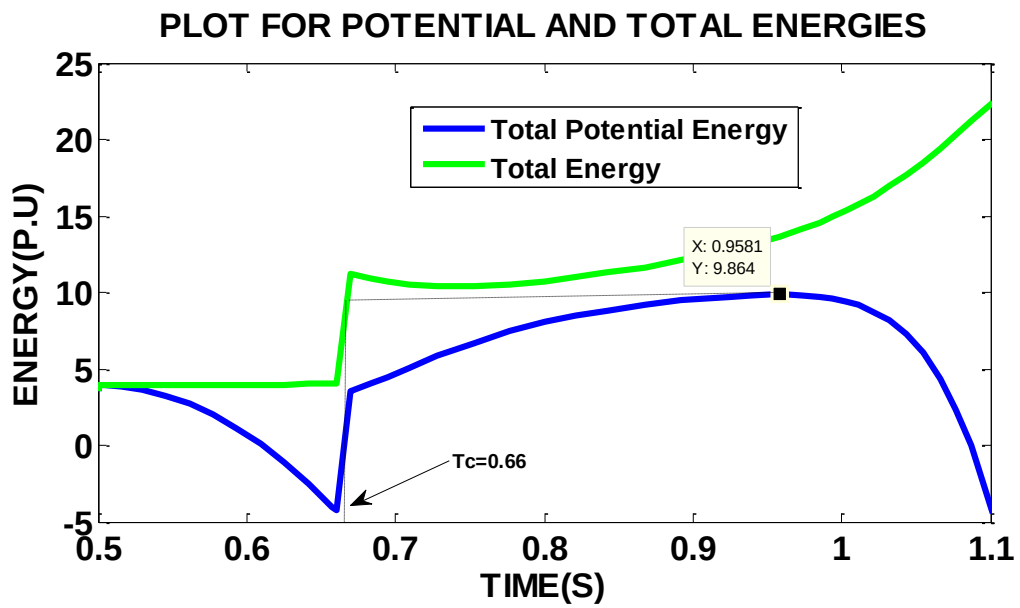

FIGURE 5.16: Critical clearing angle determination using PEBS method for system with frequency dependent loads

5.6. Simulation Results Analysis

Transient stability analysis is done on WSCC 9-bus test system and New England 39 bus test system. The structure of the network was preserved and nonlinear loads like frequency depended loads were used. The energy functions formulated in section 5.4 are used. Main observations are

- Generator rotor angles and speed variations with structure preserved models are slightly different from the conventional reduced network for same fault and for same clearing time.
- As the generator rotor angles and speed variations for SP models are slightly different from reduced models we can see the effect in total energy, kinetic energy and potential energy. We can see this small shift in energies in the figure 5.6.
- In case 2 and case 3 transient stability was done on New England 39 bus test system and on 68 bus test system with complete network preserved and employing

frequency dependent loads and generator rotor angles variations and speed are plotted in the figures

- In figure 5.9. and 5.15. Energies for the network with constant impedance loads and for the networks with frequency dependent loads were plotted. Energies with frequency dependent loads are different from constant impedance loads.
- System with frequency loads are more disturbed compared to system with constant impedance loads. Since most of the loads are frequency dependent loads, it is better to use frequency dependent loads for transient stability analysis to get accurate stability margins.
- Results obtained using structure preserving models with nonlinear loads are more realistic and accurate stability margins can be predicted.

5.7. Summary

In this Chapter, concepts of structure preserving networks are discussed and equations for structure preserving networks are derived. Also, effect of load models on the stability of the system are discussed and transient energy functions for structure preserving network with frequency dependent loads are discussed. Simulations are performed on both IEEE 3 machine 9 bus and IEEE 39 bus test systems, effect of frequency dependent loads on the system stability is discussed and critical clearing time is determined for total energy and potential energy using PEBS method.

In chapter 6, future work and conclusion made from the all chapters are discussed.

CHAPTER 6 : CONCLUSIONS AND FUTURE WORK INVERTER

In this chapter conclusions and future work of thesis are presented. Section 6.1 presents conclusions and section 6.2 presents future work.

6.1. Conclusions

In this work an investigation towards transient stability assessment using direct method are performed. Structure preserving networks with nonlinear loads are used for developing energy functions and calculating critical clearing time. The method is then compared with the time domain models. For analysis purpose IEEE standard test systems including New England 39 bus system is used. It has been observed that the proposed method provides accurate results as opposed to the conventional methods. The ability of the proposed architecture to provide energy functions for each network parts and to include nonlinear loads allows to preserve the network intact and at the same time accurately represents the transient stability analysis. Further analysis indicate that the proposed method can be employed at any power grid without much computational issues.

6.2. Future work

For future work following directions could be explored.

1. The inclusion of stochastic loads should be studied in detail.
2. Models related to nonlinear loads and stochastic generating resources should be evaluated.

3. System models with energy functions and evaluation of micro grids and other distributed energy resources such as wind farms and Photo Voltaic Systems.
4. Control architectures and designs with structure preserving stability functions could be assessed.
5. Developing transient stability models using real-time simulators.

BIBLIOGRAPHY

[1] Kundur, P., Power System Stability and Control, McGraw-Hill, Inc., New York, 1994.

[2] National Programme on Technical and Enhanced Learning, Funded by Ministry of HRD, Government of India.

[3] Definition and Classification of Power System Stability, IEEE Transactions on Power Systems, VOL. 19, NO. 2, MAY 2004.

[4] CIGRE Task Force 38.01.07 on Power System Oscillations, "Analysis and Control of Power System Oscillations," CIGRE Technical Brochure, no. 111, Dec. 1996.

[5] T. Van Cutsem and C. Vournas, Voltage Stability of Electric Power Systems. Norwell, MA: Kluwer, 1998.

[6] Hadi Saadat, Power System Analysis, Tata McGraw-Hill.

[7] A Practical Method for Power Systems Transient Stability and Security by Hussain Hassan Al Marhoon, University of New Orleans, 2008.

[8] Haque, M.H., "Equal-Area Criterion: An Extension for Multi-machine Power Systems," Generation, Transmission and Distribution, IEE Proceedings , Vol.141, NO.3, pp.191-197, May 1994.

[9] Computational Methods in Power Systems, National Programme On Technical And Enhanced Learning, Funded by Ministry of HRD, Government of India.

[10] Magnusson, P.C., "Transient Energy Method of Calculating Stability," AIEE Trans., Vol. 66, pp. 747-755, 194.

[11] Aylett, P.D., "The Energy Integral-Criterion of Transient Stability Limits of Power Systems," Proc. IEE, Vol. 105c, No. 8, pp. 527-536, September 1958.

[12] J. Hossain and H. R. Pota, Robust Control for Grid Voltage Stability: 19 High Penetration of Renewable Energy, Power Systems, DOI: 10.1007/978-981-287-116-9_2, Springer Science+Business Media Singapore 2014.

[13] Power System Transient Stability Analysis Using Transient Energy Function Method by A.A.Fouad/Vijay Vittal.

[14] Power System Stability and Dynamics by K.R.Padiyar.

[15] Michel, A., Fouad, A., Vittal, V., "Power System Transient Stability Using Individual Machine Energy Functions," Circuits and Systems, IEEE Transactions on, vol.30, no.5, pp. 266- 276, May 1983.

[16] P28,http://www.scribd.com/doc/49081324/26/Western-System-Coordinating-Council-WSCC-3-Machines-9-Bus-system.

[17] Parametric Approach to Steady-State Stability Analysis of Power Systems by Rajeev Kumar Ranjan.

[18] Sauer, P. W., Pai, M. A., Power System Dynamic and Stability, Prentice-Hall, Inc. New Jersey, 1998.

[19] Magnusson, P.C., "Transient Energy Method of Calculating Stability," AIEE Trans., Vol. 66, pp. 747-755, 1947.

[20] Da-Zhong Fang, Chung, T.S., Yao Zhang, Wennan Song, "Transient Stability Limit Conditions Analysis Using a Corrected Transient Energy Function Approach," Power Systems, IEEE Transactions on, vol.15, no.2, pp.804-810, May 2000.

[21] Rastgoufard, P., Yazdankhah, A., Schlueter, R.A., "Multi-Machine Equal Area Based Power System Transient Stability Measure," IEEE Transactions on Power Systems, vol.3, no.1, pp.188-196, Feb 1988.

[22] Athay, T., Podmore, R., Virmani, S., "A Practical Method for the Direct Analysis of Transient Stability," IEEE Transactions on Power Apparatus and Systems, vol.PAS-98, no.2, pp.573-584, March 1979.

[23] Structure Preserving Energy Functions in Power Systems by K.R.Padiyar.

[24] IEEE Transactions on Power Apparatus and Systems, Vol. PAS-100, No. 1, January 1981 A Structure Preserving Model For Power System Stability Analysis A.R. Bergen, Ilember, IEEE D.J. Hill, Member, IEEE.

[25] Dynamics and Control of Electric Power Systems Lecture 227-0528-00, ITET ETH Goran Andersson EEH - Power Systems Laboratory ETH Z¨urich February 2012.

[26] M. A. Pai, Energy Function Analysis for Power System Stability. Norwell, MA: Kluwer, 1989.

[27] A.H. EL-ABIAD and Nagappan, "Transient Stability Studies of Multi-Machine Power Systems"

[28] Definition and Classification of Power System Stability, IEEE/CIGRE Joint Task Force on Stability Terms and Definitions.

[29] M. Ribbens-Pavella, "Transient Stability of Multi-machine Power Systems by Lyapunov's Direct Method 71 CP17-PWR", IEEE Winter Power Meeting, 1971.

[30] M. A. Pai, Computer Techniques in Power Systems Analysis, 1979 :Tata-McGraw Hill.

[31] Behera, A.K. 1988. Transient Stability Analysis Of Multi-Machine Power Systems Using Detailed Machine Models. PhD Thesis, University of Illinois at Urbana-Champaign.

[32] Area-Based COI-Referred Rotor Angle Index for Transient Stability Assessment and Control of Power Systems by Noor Izzri Abdul Wahab and Azah Mohamed.

[33] Direct Stability Analysis of Electric Power Systems Using Energy Functions: Theory, Applications, and Perspective by Hsiao-Dong Chiang, Senior Member, IEEE, Chia-Chi Chu, Student Member, IEEE, and Gerry Cauley, Senior Member, IEEE.

[34] C.A. Desoer and E.S. Kuh, Basic Circuit Theory, 1969 :McGraw-Hill.

[35] A.R. Bergen and G. Gross on Multi-Machine Power System Representations, 1972.

[36] L.B. Jocia, M. Ribbens-Pavella and D.D. Siljak "Multi-Machine Power Systems: Stability, Decomposition, and Aggregation", IEEE Trans. Automatic Control, Vol. AC-23, pp.325 -332 1978 .

[37] Bergen, A.R., Vittal, V., Power Systems Analysis, Prentice-Hall, Inc, New Jersey, 2nd edition, 2000.

[38] N. A. Tsolas, A. Arapostathis, and P. P. Varaiya, "A Structure Preserving Function For Power System Transient Stability Analysis," IEEE Trans. Circuits Syst., vol. CAS-32, no. 10, pp. 1041–1049, Oct. 1985.

[39] M. K. Khedkar, G. M. Dhole, and V. G. Neve, "Transient Stability Analysis By Transient Energy Function Method: Closest and Controlling Unstable Equilibrium Point Approach," IE (I) Journal, vol. 85, pp. 83–88, Sep. 2004.

[40] Large Disturbance Voltage Stability Assessment Using Extended Lyapunov Function and Considering Voltage Dependent Active Loads R.B.L. Guedes, F.H.J.R. Silva, L.F.C. Alberto, and N.G. Bretas.

[41] Anderson, Fouad, Power System Stability and Control, A John Wiley & Sons, Inc., Publication.

[42] Peter W. Sauer and M.A.Pai, Power System Dynamics and Stability, Prentice Hall.

[43] Structure Preserving Direct Methods For Transient Stability Analysis of Power Systems, Th. Van Cutsem and M.Ribbens-Pavella, Proceedings of 24th Conference on Decision and Control, FL, December 1985.

[44] D.J. Hill, A.R. Bergen, Stability Analysis of Multi-machine Power Network with Linear Frequency Dependent Loads. IEEE Trans. on CAS, Vol. CAS-299, No. 12, Dec. 1982, pp. 840-848.

[45] N Narasimhamurti, M.R., Musavi, A General Energy Function for Transient Stability Analysis. IEEE Trans. on CAS, Vol. CAS-31, No.7, July 1984, PP. 637-645.

[46] Steinmetz, C.P., "Power Control and Stability of Electric Generating Stations," AIEE Trans.,Vol. XXXIX, no.2, pp.1215-1287, July 1920.

[47] Stability Control Using PEBS Method and Analytical Sensitivity of The Transient Energy Margin, H. Song, Student Member, IEEE, and M. Kezunovic, Fellow, IEEE.

[48] Fast Transient Stability Assessment Using Corrective PEBS Method, Pave1 Omahen Electro institute "Milan Vidmar", 61000 Ljubljana, Hajdrihova 2. Yugoslavia.

[49] Foundations of the Potential Energy Boundary Surface Method for Power System Transient Stability Analysis, Hsiao-Dong Chiang, Felix F. Wu, Senior Member, IEEE, and Pravin P. Vauiya, Fellow, IEEE.

[50] John J. Grainger, William D. Stevenson, JR., Power System Analysis., McGraw-Hill.

APPENDIX A: BUS DATA

New England 39 Bus Test System Data:

Generator Data:

Unit No.	H	R_a	x'_d	x'_q	x_d	x_q	T'_{do}	T'_{qo}	x_l	x''	T''_{do}	T''_{qo}
1	500.0	0	0.006	0.008	0.02	0.019	7.0	0.7	0.003	0.004	0.05	0.035
2	30.3	0	0.0697	0.170	0.295	0.282	6.56	1.5	0.035	0.050	0.05	0.035
3	35.8	0	0.0531	0.0876	0.2495	0.237	5.7	1.5	0.0304	0.045	0.05	0.035
4	28.6	0	0.0436	0.166	0.262	0.258	5.69	1.5	0.0295	0.035	0.05	0.035
5	26.0	0	0.132	0.166	0.67	0.62	5.4	0.44	0.054	0.089	0.05	0.035
6	34.8	0	0.05	0.0814	0.254	0.241	7.3	0.4	0.0224	0.040	0.05	0.035
7	26.4	0	0.049	0.186	0.295	0.292	5.66	1.5	0.0322	0.044	0.05	0.035
8	24.3	0	0.057	0.0911	0.290	0.280	6.7	0.41	0.028	0.045	0.05	0.035
9	34.5	0	0.057	0.0587	0.2106	0.205	4.79	1.96	0.0298	0.045	0.05	0.035
10	42.0	0	0.031	0.050	0.1	0.069	10.2	0.0	0.0125	0.025	0.05	0.035

Lines and Transformer Data:

Line Data					Transformer Tap	
From Bus	To Bus	R	X	B	Magnitude	Angle
1	2	0.0035	0.0411	0.6987	0.000	0.00
1	39	0.0010	0.0250	0.7500	0.000	0.00
2	3	0.0013	0.0151	0.2572	0.000	0.00
2	25	0.0070	0.0086	0.1460	0.000	0.00
3	4	0.0013	0.0213	0.2214	0.000	0.00
3	18	0.0011	0.0133	0.2138	0.000	0.00
4	5	0.0008	0.0128	0.1342	0.000	0.00
4	14	0.0008	0.0129	0.1382	0.000	0.00
5	6	0.0002	0.0026	0.0434	0.000	0.00
5	8	0.0008	0.0112	0.1476	0.000	0.00
6	7	0.0006	0.0092	0.1130	0.000	0.00
6	11	0.0007	0.0082	0.1389	0.000	0.00
7	8	0.0004	0.0046	0.0780	0.000	0.00
8	9	0.0023	0.0363	0.3804	0.000	0.00
9	39	0.0010	0.0250	1.2000	0.000	0.00
10	11	0.0004	0.0043	0.0729	0.000	0.00
10	13	0.0004	0.0043	0.0729	0.000	0.00
13	14	0.0009	0.0101	0.1723	0.000	0.00
14	15	0.0018	0.0217	0.3660	0.000	0.00
15	16	0.0009	0.0094	0.1710	0.000	0.00
16	17	0.0007	0.0089	0.1342	0.000	0.00
16	19	0.0016	0.0195	0.3040	0.000	0.00
16	21	0.0008	0.0135	0.2548	0.000	0.00
16	24	0.0003	0.0059	0.0680	0.000	0.00
17	18	0.0007	0.0082	0.1319	0.000	0.00
17	27	0.0013	0.0173	0.3216	0.000	0.00
21	22	0.0008	0.0140	0.2565	0.000	0.00
22	23	0.0006	0.0096	0.1846	0.000	0.00
23	24	0.0022	0.0350	0.3610	0.000	0.00
25	26	0.0032	0.0323	0.5130	0.000	0.00
26	27	0.0014	0.0147	0.2396	0.000	0.00
26	28	0.0043	0.0474	0.7802	0.000	0.00

26	29	0.0057	0.0625	1.0290	0.000	0.00
28	29	0.0014	0.0151	0.2490	0.000	0.00
12	11	0.0016	0.0435	0.0000	1.006	0.00
12	13	0.0016	0.0435	0.0000	1.006	0.00
6	31	0.0000	0.0250	0.0000	1.070	0.00
10	32	0.0000	0.0200	0.0000	1.070	0.00
19	33	0.0007	0.0142	0.0000	1.070	0.00
20	34	0.0009	0.0180	0.0000	1.009	0.00
22	35	0.0000	0.0143	0.0000	1.025	0.00
23	36	0.0005	0.0272	0.0000	1.000	0.00
25	37	0.0006	0.0232	0.0000	1.025	0.00
2	30	0.0000	0.0181	0.0000	1.025	0.00
29	38	0.0008	0.0156	0.0000	1.025	0.00
19	20	0.0007	0.0138	0.0000	1.060	0.00

Voltage and Power Set Points:

Bus	Type	Voltage [p.u]	Load		Generator		
			MW	MVar	MW	MVar	Unit No.
1	PQ	-	0.0	0.0	0.0	0.0	
2	PQ	-	0.0	0.0	0.0	0.0	
3	PQ	-	322.0	2.4	0.0	0.0	
4	PQ	-	500.0	184.0	0.0	0.0	
5	PQ	-	0.0	0.0	0.0	0.0	
6	PQ	-	0.0	0.0	0.0	0.0	
7	PQ	-	233.8	84.0	0.0	0.0	
8	PQ	-	522.0	176.0	0.0	0.0	
9	PQ	-	0.0	0.0	0.0	0.0	
10	PQ	-	0.0	0.0	0.0	0.0	
11	PQ	-	0.0	0.0	0.0	0.0	
12	PQ	-	7.5	88.0	0.0	0.0	
13	PQ	-	0.0	0.0	0.0	0.0	
14	PQ	-	0.0	0.0	0.0	0.0	
15	PQ	-	320.0	153.0	0.0	0.0	
16	PQ	-	329.0	32.3	0.0	0.0	
17	PQ	-	0.0	0.0	0.0	0.0	
18	PQ	-	158.0	30.0	0.0	0.0	
19	PQ	-	0.0	0.0	0.0	0.0	
20	PQ	-	628.0	103.0	0.0	0.0	
21	PQ	-	274.0	115.0	0.0	0.0	
22	PQ	-	0.0	0.0	0.0	0.0	
23	PQ	-	247.5	84.6	0.0	0.0	
24	PQ	-	308.6	-92.0	0.0	0.0	
25	PQ	-	224.0	47.2	0.0	0.0	
26	PQ	-	139.0	17.0	0.0	0.0	
27	PQ	-	281.0	75.5	0.0	0.0	
28	PQ	-	206.0	27.6	0.0	0.0	
29	PQ	-	283.5	26.9	0.0	0.0	
30	PV	1.0475	0.0	0.0	250.0	-	Gen10
31	PV	0.9820	9.2	4.6	-	-	Gen2
32	PV	0.9831	0.0	0.0	650.0	-	Gen3
33	PV	0.9972	0.0	0.0	632.0	-	Gen4
34	PV	1.0123	0.0	0.0	508.0	-	Gen5
35	PV	1.0493	0.0	0.0	650.0	-	Gen6
36	PV	1.0635	0.0	0.0	560.0	-	Gen7
37	PV	1.0278	0.0	0.0	540.0	-	Gen8

38	PV	1.0265	0.0	0.0	830.0	-	Gen9
39	PV	1.0300	1104.0	250.0	1000.0	-	Gen1

NETS-NYPS 68 Bus Test System Data:

Generator Data:

Unit No.	R_a	X'_d	H
1	0	0.0310	42
2	0	0.0697	30.2
3	0	0.0531	35.8
4	0	0.0436	28.6
5	0	0.0660	26
6	0	0.0500	34.8
7	0	0.0490	26.4
8	0	0.0570	24.3
9	0	0.0570	34.5
10	0	0.0457	31
11	0	0.0180	28.2
12	0	0.0310	92.3
13	0	0.0055	240
14	0	0.0029	300
15	0	0.0029	300
16	0	0.0071	225

Line Data:

From bus	To bus	R (p.u)	X (p.u)	B/2 (p.u)	Transformer tap setting
1	54	0	0.0181	0	1.025
2	58	0	0.025	0	1.07
3	62	0	0.02	0	1.07
4	19	0.0007	0.0142	0	1.07
5	20	0.0009	0.018	0	1.009
6	22	0	0.0143	0	1.025
7	23	0.0005	0.0272	0	1
8	25	0.0006	0.0232	0	1.025
9	29	0.0008	0.0156	0	1.025
10	31	0	0.026	0	1.04
11	32	0	0.013	0	1.04
12	36	0	0.0075	0	1.04
13	17	0	0.0033	0	1.04
14	41	0	0.0015	0	1
15	42	0	0.0015	0	1
16	18	0	0.003	0	1
17	36	0.0005	0.0045	0.16	1
18	49	0.0076	0.1141	0.8	1
18	50	0.0012	0.0288	1.03	1
19	68	0.0016	0.0195	0.152	1
20	19	0.0007	0.0138	0	1.06
21	68	0.0008	0.0135	0.1274	1
22	21	0.0008	0.014	0.1283	1
23	22	0.0006	0.0096	0.0923	1
24	23	0.0022	0.035	0.1805	1

24	68	0.0003	0.0059	0.034	1
25	54	0.007	0.0086	0.073	1
26	25	0.0032	0.0323	0.2655	1
27	37	0.0013	0.0173	0.1608	1
27	26	0.0014	0.0147	0.1198	1
28	26	0.0043	0.0474	0.3901	1
29	26	0.0057	0.0625	0.5145	1
29	28	0.0014	0.0151	0.1245	1
30	53	0.0008	0.0074	0.24	1
30	61	0.001	0.0092	0.29	1
31	30	0.0013	0.0187	0.1665	1
31	53	0.0016	0.0163	0.125	1
32	30	0.0024	0.0288	0.244	1
33	32	0.0008	0.0099	0.084	1
34	33	0.0011	0.0157	0.101	1
34	35	0.0001	0.0074	0	0.946
36	34	0.0033	0.0111	0.725	1
36	61	0.0011	0.0098	0.34	1
37	68	0.0007	0.0089	0.0671	1
38	31	0.0011	0.0147	0.1235	1
38	33	0.0036	0.0444	0.3465	1
40	41	0.006	0.084	1.575	1
40	48	0.002	0.022	0.64	1
41	42	0.004	0.06	1.125	1
42	18	0.004	0.06	1.125	1
43	17	0.0005	0.0276	0	1
44	39	0	0.0411	0	1
44	43	0.0001	0.0011	0	1
45	35	0.0007	0.0175	0.695	1
45	39	0	0.0839	0	1
45	44	0.0025	0.073	0	1
46	38	0.0022	0.0284	0.215	1
47	53	0.0013	0.0188	0.655	1
48	47	0.0013	0.0134	0.4	1
49	46	0.0018	0.0274	0.135	1
51	45	0.0004	0.0105	0.36	1
51	50	0.0009	0.0221	0.81	1
52	37	0.0007	0.0082	0.0659	1
52	55	0.0011	0.0133	0.1069	1
54	53	0.0035	0.0411	0.3493	1
55	54	0.0013	0.0151	0.1286	1
56	55	0.0013	0.0213	0.1107	1
57	56	0.0008	0.0128	0.0671	1
58	57	0.0002	0.0026	0.0217	1
59	58	0.0006	0.0092	0.0565	1
60	57	0.0008	0.0112	0.0738	1
60	59	0.0004	0.0046	0.039	1
61	60	0.0023	0.0363	0.1902	1
63	58	0.0007	0.0082	0.0694	1
63	62	0.0004	0.0043	0.0365	1
63	64	0.0016	0.0435	0	1.06
65	62	0.0004	0.0043	0.0365	1
65	64	0.0016	0.0435	0	1.06
66	56	0.0008	0.0129	0.0691	1
66	65	0.0009	0.0101	0.0862	1
67	66	0.0018	0.0217	0.183	1
68	67	0.0009	0.0094	0.0855	1
27	53	0.032	0.32	0.205	1
69	1	0	0.031	0	1

70	2	0	0.0697	0	1
71	3	0	0.0531	0	1
72	4	0	0.0436	0	1
73	5	0	0.066	0	1
74	6	0	0.05	0	1
75	7	0	0.049	0	1
76	8	0	0.057	0	1
77	9	0	0.057	0	1
78	10	0	0.0457	0	1
79	11	0	0.018	0	1
80	12	0	0.031	0	1
81	13	0	0.0055	0	1
82	14	0	0.0029	0	1
83	15	0	0.0029	0	1
84	16	0	0.0071	0	1

Bus Data:

Bus no.	Bus code	V(p.u)	Delta	$P_{L(M.W)}$	$Q_{L(Mvar)}$	$P_{G(M.W)}$	$Q_{G(Mvar)}$	$Q_{min(Mvar)}$	$Q_{max(Mvar)}$
1	2	1.045	0	0	0	250	0	-999	999
2	2	0.98	0	0	0	545	0	-999	999
3	2	0.983	0	0	0	650	0	-999	999
4	2	0.997	0	0	0	632	0	-999	999
5	2	1.011	0	0	0	505	0	-999	999
6	2	1.05	0	0	0	700	0	-999	999
7	2	1.063	0	0	0	560	0	-999	999
8	2	1.03	0	0	0	540	0	-999	999
9	2	1.025	0	0	0	800	0	-999	999
10	2	1.01	0	0	0	500	0	-999	999
11	2	1	0	0	0	1000	0	-999	999
12	2	1.0156	0	0	0	1350	0	-999	999
13	2	1.011	0	0	0	3591	0	-999	999
14	2	1	0	0	0	1785	0	-999	999
15	2	1	0	0	0	1000	0	-999	999
16	1	1	0	0	0	40	0	0	0
17	0	1	0	6000	300	0	0	0	0
18	0	1	0	2470	123	0	0	0	0
19	0	1	0	0	0	0	0	0	0
20	0	1	0	680	103	0	0	0	0
21	0	1	0	274	115	0	0	0	0
22	0	1	0	0	0	0	0	0	0
23	0	1	0	248	85	0	0	0	0
24	0	1	0	309	-92	0	0	0	0
25	0	1	0	224	47	0	0	0	0
26	0	1	0	139	17	0	0	0	0
27	0	1	0	281	76	0	0	0	0
28	0	1	0	206	28	0	0	0	0
29	0	1	0	284	27	0	0	0	0
30	0	1	0	0	0	0	0	0	0
31	0	1	0	0	0	0	0	0	0
32	0	1	0	0	0	0	0	0	0
33	0	1	0	112	0	0	0	0	0
34	0	1	0	0	0	0	0	0	0
35	0	1	0	0	0	0	0	0	0
36	0	1	0	102	-19.46	0	0	0	0
37	0	1	0	0	0	0	0	0	0
38	0	1	0	0	0	0	0	0	0

39	0	1	0	267	12.6	0	0	0	0
40	0	1	0	65.63	23.53	0	0	0	0
41	0	1	0	1000	250	0	0	0	0
42	0	1	0	1150	250	0	0	0	0
43	0	1	0	0	0	0	0	0	0
44	0	1	0	267.55	4.84	0	0	0	0
45	0	1	0	208	21	0	0	0	0
46	0	1	0	150.7	28.5	0	0	0	0
47	0	1	0	203.12	32.59	0	0	0	0
48	0	1	0	241.2	2.2	0	0	0	0
49	0	1	0	164	29	0	0	0	0
50	0	1	0	100	-147	0	0	0	0
51	0	1	0	337	-122	0	0	0	0
52	0	1	0	158	30	0	0	0	0
53	0	1	0	252.7	118.56	0	0	0	0
54	0	1	0	0	0	0	0	0	0
55	0	1	0	322	2	0	0	0	0
56	0	1	0	200	73.6	0	0	0	0
57	0	1	0	0	0	0	0	0	0
58	0	1	0	0	0	0	0	0	0
59	0	1	0	234	84	0	0	0	0
60	0	1	0	208.8	70.8	0	0	0	0
61	0	1	0	104	125	0	0	0	0
62	0	1	0	0	0	0	0	0	0
63	0	1	0	0	0	0	0	0	0
64	0	1	0	9	88	0	0	0	0
65	0	1	0	0	0	0	0	0	0
66	0	1	0	0	0	0	0	0	0
67	0	1	0	320	153	0	0	0	0
68	0	1	0	329	32	0	0	0	0

Power Flow Result of NETS-NYPS 68 BUS TEST SYSTEM

Bus no.	V(p.u)	Delta(deg)	P_L	Q_L	P_G	Q_G
1	1.045	-8.896	0	0	250	194.963
2	0.98	-0.924	0	0	545	69.646
3	0.983	1.672	0	0	650	80.453
4	0.997	1.729	0	0	632	0.128
5	1.011	-0.566	0	0	505	116.505
6	1.05	3.903	0	0	700	254.314
7	1.063	6.092	0	0	560	290.733
8	1.03	-2.779	0	0	540	48.521
9	1.025	2.714	0	0	800	59.577
10	1.01	-9.591	0	0	500	-18.428
11	1	-7.169	0	0	1000	4.238
12	1.016	-22.564	0	0	1350	277.618
13	1.011	-28.583	0	0	3591	882.165
14	1	10.982	0	0	1785	46.334
15	1	0.029	0	0	1000	75.301
16	1	0	0	0	3379.757	63.021
17	0.95	-35.955	6000	300	0	0
18	1.003	-5.8	2470	123	0	0
19	0.932	-4.202	0	0	0	0
20	0.981	-5.813	680	103	0	0
21	0.96	-6.993	274	115	0	0
22	0.994	-1.74	0	0	0	0
23	0.996	-2.1	248	85	0	0

24	0.959	-9.815	309	-92	0	0
25	0.998	-9.937	224	47	0	0
26	0.987	-10.957	139	17	0	0
27	0.968	-12.795	281	76	0	0
28	0.99	-7.435	206	28	0	0
29	0.992	-4.484	284	27	0	0
30	0.977	-19.64	0	0	0	0
31	0.985	-17.4	0	0	0	0
32	0.97	-15.178	0	0	0	0
33	0.975	-19.695	112	0	0	0
34	0.981	-26.051	0	0	0	0
35	1.044	-27.025	0	0	0	0
36	0.961	-28.758	102	-19.46	0	0
37	0.956	-11.726	0	0	0	0
38	0.992	-18.694	0	0	0	0
39	0.992	-39.218	267	12.6	0	0
40	1.045	-13.591	65.63	23.53	0	0
41	1	9.447	1000	250	0	0
42	0.999	-0.832	1150	250	0	0
43	0.977	-37.837	0	0	0	0
44	0.978	-37.915	267.55	4.84	0	0
45	1.048	-29.301	208	21	0	0
46	0.998	-20.45	150.7	28.5	0	0
47	1.019	-19.432	203.12	32.59	0	0
48	1.035	-18.316	241.2	2.2	0	0
49	1.005	-19.751	164	29	0	0
50	1.061	-19.015	100	-147	0	0
51	1.064	-27.232	337	-122	0	0
52	0.955	-12.772	158	30	0	0
53	0.987	-18.87	252.7	118.56	0	0
54	0.986	-11.476	0	0	0	0
55	0.957	-13.156	322	2	0	0
56	0.921	-11.898	200	73.6	0	0
57	0.91	-11.153	0	0	0	0
58	0.909	-10.342	0	0	0	0
59	0.904	-13.25	234	84	0	0
60	0.906	-13.976	208.8	70.8	0	0
61	0.956	-23.16	104	125	0	0
62	0.912	-7.252	0	0	0	0
63	0.91	-8.31	0	0	0	0
64	0.837	-8.317	9	88	0	0
65	0.913	-8.125	0	0	0	0
66	0.919	-10.13	0	0	0	0
67	0.928	-11.368	320	153	0	0
68	0.948	-10.01	329	32	0	0

APPENDIX B: GRAPHS

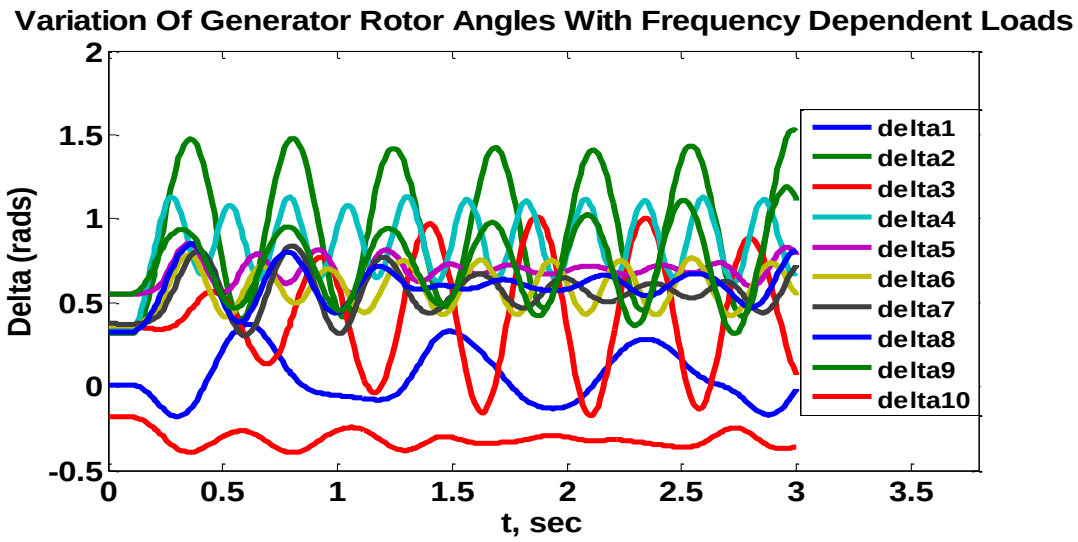

Generator rotor angle variation with frequency dependent loads versus time

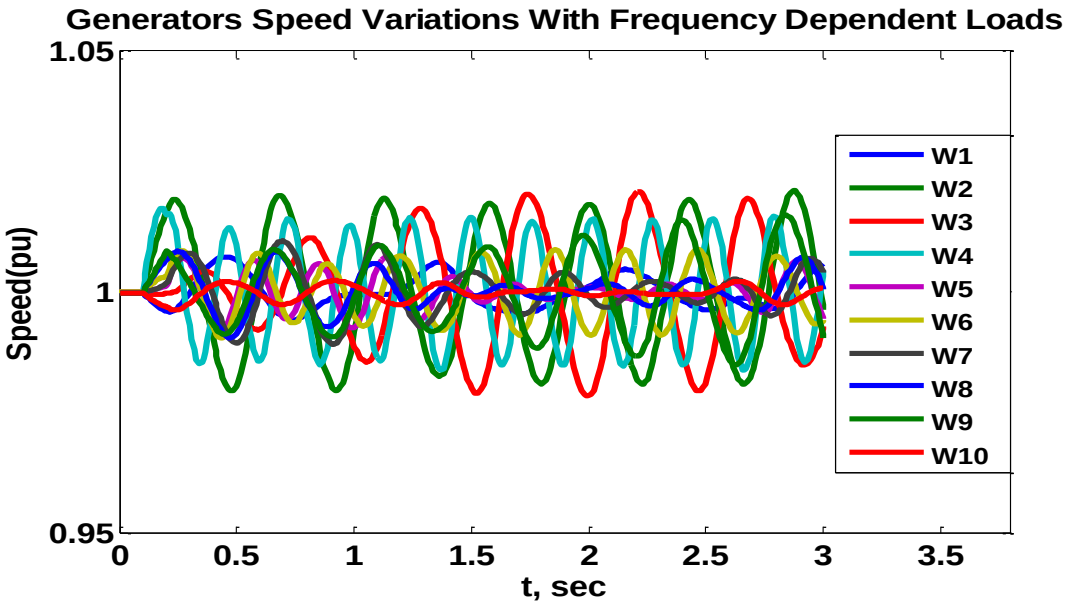

Generator speed variation with frequency dependent loads versus time